National Center for Theoretical Sciences

Error Analysis of a Stabilized Finite Element Method for the Generalized Stokes Problem

Huo-Yuan Duan, Po-Wen Hsieh, Roger Choon Ee Tan, and Suh-Yuh Yang

NCTS/Math
Technical Report
2018-002

Journal of Computational Mathematics
Vol.xx, No.x, 2018, 1–38.

http://www.global-sci.org/jcm
doi:??

ERROR ANALYSIS OF A STABILIZED FINITE ELEMENT METHOD FOR THE GENERALIZED STOKES PROBLEM*

Huo-Yuan Duan
School of Mathematics and Statistics, Wuhan University, Wuhan, China
Email: hyduan.math@whu.edu.cn
Po-Wen Hsieh
Department of Applied Mathematics, National Chung Hsing University, Taichung City, Taiwan
Email: pwhsieh@nchu.edu.tw
Roger C. E. Tan
Department of Mathematics, National University of Singapore, Singapore
Email: scitance@nus.edu.sg
Suh-Yuh Yang
Department of Mathematics, National Central University, Taoyuan City, Taiwan
and National Center for Theoretical Sciences, Taipei City, Taiwan
Email: syyang@math.ncu.edu.tw

Abstract

This paper is devoted to the establishment of sharper *a priori* stability and error estimates of a stabilized finite element method proposed by Barrenechea and Valentin [3] for solving the generalized Stokes problem, which involves a viscosity ν and a reaction constant σ. With the establishment of sharper stability estimates and the help of *ad hoc* finite element projections, we can explicitly establish the dependence of error bounds of velocity and pressure on the viscosity ν, the reaction constant σ, and the mesh size h. Our analysis reveals that the viscosity ν and the reaction constant σ respectively act in the numerator position and the denominator position in the error estimates of velocity and pressure in standard norms without any weights. Consequently, the stabilization method is indeed suitable for the generalized Stokes problem with a small viscosity ν and a large reaction constant σ. The sharper error estimates agree very well with the numerical results.

Mathematics subject classification: 65N12, 65N15, 65N30, 76M10.
Key words: generalized Stokes equations, stabilized finite element method, error estimates.

1. Introduction and Preliminaries

Let Ω be an open bounded polygonal domain in $\mathbb{R}^d$ ($d = 2$ or 3) with boundary $\partial\Omega$. In this paper, we will study the stabilized C^0 finite element approximations, proposed by Barrenechea and Valentin in [3], to the following system of generalized Stokes equations with the homogeneous velocity boundary condition:

$$\begin{cases} \sigma \boldsymbol{u} - \nu\Delta\boldsymbol{u} + \nabla p = \boldsymbol{f} & \text{in } \Omega, \\ \nabla\cdot\boldsymbol{u} = 0 & \text{in } \Omega, \\ \boldsymbol{u} = \boldsymbol{0} & \text{on } \partial\Omega, \end{cases} \tag{1.1}$$

* Received August 07, 2017 / Revised version received February 10, 2018 / Accepted May 21, 2018 /

where $\boldsymbol{u} : \overline{\Omega} \to \mathbb{R}^d$ is the velocity field and $p : \overline{\Omega} \to \mathbb{R}$ is the pressure; $\nu > 0$ is the viscosity constant; $\sigma > 0$ is the reaction constant; and $\boldsymbol{f} : \Omega \to \mathbb{R}^d$ is a given source-like function in $(L^2(\Omega))^d$.

In general, the finite element approach for solving problem (1.1) is posed as a velocity-pressure mixed formulation in the standard Galerkin method. However, it is well known that, for stable and optimally accurate approximations, the pair $(\boldsymbol{V}_h, Q_h)$ of finite element spaces for the mixed formulation must satisfy the so-called *inf-sup condition*,

$$\sup_{\boldsymbol{v} \in \boldsymbol{V}_h} \frac{(\nabla \cdot \boldsymbol{v}, q)}{\|\boldsymbol{v}\|_1} \geq c\|q\|_0 \quad \forall\, q \in Q_h, \tag{1.2}$$

see, e.g., [8], [10], and [25]. This condition prevents the use of standard equal order $\mathcal{C}^0$ finite element spaces for velocity and pressure with respect to the same triangulation that are the most attractive from the viewpoint of implementation. In order to circumvent the inf-sup condition, a class of so-called stabilized finite element methods (FEMs) has been developed and intensively studied for more than thirty years, see, e.g., [6], [7], [9], [11], [12], [15], [21], [22], [26], [27], [32], [33], [35], and [39]. The stabilized FEMs are formed by adding to the discrete mixed formulation of the generalized Stokes problem (1.1) with some consistent variational terms, relating to the residuals of the partial differential equations (cf. [14], [16], [19], [20], [23], [30], [31], [36], and [37]). With suitable stabilization parameters, the stabilized FEMs are successful in circumventing the above inf-sup condition.

Typically, the generalized Stokes problem (1.1) may arise from the time discretization (cf. [38]) of transient Stokes equations or full Navier-Stokes equations by means of an operator splitting technique, where the reaction constant is given by $\sigma = c(\delta t)^{-1}$ and δt is the time step. For problems involving fast chemical reactions, a small time step, namely a large σ, is needed in order to account for the stiffness due to the fast reaction. However, in the context of stabilization methods, it has been observed that the pressure instabilities may be caused as the time step δt becomes small compared to the spatial grid size h. Therefore, in recent years, there has been increasingly a great deal of attention on the theoretical and computational studies of small time-step instabilities when implicit, finite difference time integration is applied in combination with finite element stabilization in the spatial semi-discretization, see, e.g., [4], [5], [14], [17], [19], and [31]. Nowadays, it has been extensively recognized that the stabilized FEMs are most effective in dealing with the instability in the finite element solution.

In [3], Barrenechea and Valentin proposed a stabilized FEM for solving the generalized Stokes problem (1.1) in 2D. The unusual feature of this stabilized FEM is that it involves the subtraction of the stabilization term $\sum_{K \in \mathcal{T}_h} \tau_K (\sigma \boldsymbol{u}_h, \sigma \boldsymbol{v})_{0,K}$ from the original discrete mixed finite element formulation. Numerical results provided in [3] show that the proposed method can achieve high accuracy and stability. More remarkably, it has been numerically verified in [3] that for a fixed small viscosity ν, the H^1 errors of the resulting finite element solutions of velocity appear to be uniform in the reaction coefficient σ when σ is large enough.

In this paper, with the help of analysis of the finite element projections for velocity and pressure, together with a trick using a function $\xi(\cdot)$ of the ratio between ν and σh_K^2, we are able to derive sharper error estimates for the Barrenechea-Valentin stabilized $\mathcal{C}^0$ FEM that will be briefly stated at the end of this section. We first establish two sharper stability estimates, and then establish the explicit dependence of the error bounds on the viscosity ν, the reaction constant σ, and the mesh size h. The significant new findings in our analysis can be summarized as follows. The analysis reveals that the viscosity constant ν and the reaction constant

σ respectively act in the numerator position and the denominator position in the error estimates of velocity and pressure in standard norms without any weights. In particular, up to the regularity-norms of the exact solution pair $(\boldsymbol{u}, p)$, we can find that the H^1 semi-norm error of velocity is independent of the viscosity ν and the H^1 semi-norm error of pressure is independent of the reaction constant σ. Moreover, in a convex polygonal domain Ω, we show that the L^2 norm error estimates of velocity behave in the same manner as those of H^1 semi-norm error estimates with respect to σ and ν, by one order higher with respect to the mesh size h. We emphasize again that all the error estimates are measured in the standard H^1 semi-norm and L^2 norm without any weights of σ, ν and h. To the authors' knowledge, for example, the commonly known H^1 norm error estimates in the literature for the velocity are measured in the $\sqrt{\nu}$-weighted H^1 norm (e.g., see [24] and [40]). Consequently, our analysis proves that the stabilization method proposed in [3] is indeed particularly suitable for the generalized Stokes problem with small ν and large σ. The above theoretical results agree very well with the numerical results reported in [3]. In this paper, further numerical results will be presented to illustrate the theoretical results obtained.

In the rest of this section, we will review briefly the stabilized FEM proposed in [3] and the results of stability and error estimates obtained therein. Let $\{\mathcal{T}_h\}_{0<h\leq 1}$ be a family of triangulations of Ω, consisting of triangles if $d = 2$ or tetrahedra if $d = 3$ (cf. [13]). The mesh size h is defined as $h = \max\{h_K : K \in \mathcal{T}_h\}$, where h_K denotes the diameter of element K. We always assume that the family $\{\mathcal{T}_h\}_{0<h\leq 1}$ of triangulations is shape-regular (see [8], [18]), i.e., there exists a constant $\alpha > 0$, independent of h and K, such that $h_K \leq \alpha\rho_K$ for all $K \in \mathcal{T}_h$ and $\mathcal{T}_h \in \{\mathcal{T}_h\}_{0<h\leq 1}$, where ρ_K is the supremum of diameters of the balls inscribed in K. As usual, with a nonnegative integer l, we denote by $(\cdot,\cdot)_{l,D}$, $\|\cdot\|_{l,D}$ and $|\cdot|_{l,D}$ the associated inner product, norm and semi-norm in $H^l(D)$, respectively, where D is a given subset of Ω. When $D = \Omega$, we briefly write $(\cdot,\cdot)_{l,\Omega} = (\cdot,\cdot)_l$ for $l \geq 1$ and $(\cdot,\cdot)_{0,\Omega} = (\cdot,\cdot)$ if $l = 0$, and $\|\cdot\|_{l,\Omega} = \|\cdot\|_l$ for $l \geq 0$. In the case $l = 0$, since $\|\cdot\|_{0,D} = |\cdot|_{0,D}$, we use $\|\cdot\|_{0,D}$ to denote the L^2 norm on D.

Let $\boldsymbol{V}_h \subset (H_0^1(\Omega))^d$ and $Q_h \subset H^1(\Omega) \cap L_0^2(\Omega)$ be the finite element spaces of velocity and pressure, respectively, where $L_0^2(\Omega) = \{q \in L^2(\Omega) : \int_\Omega q = 0\}$. For $d = 2$ and the triangulation $\mathcal{T}_h$ is composed of triangles, Barrenechea and Valentin proposed and analyzed a stabilized FEM in [3] for the generalized Stokes problem (1.1) as follows: *Find* $(\boldsymbol{u}_h, p_h) \in \boldsymbol{V}_h \times Q_h$ *such that*

$$\boldsymbol{B}^{BV}((\boldsymbol{u}_h, p_h), (\boldsymbol{v}, q)) = \boldsymbol{F}^{BV}(\boldsymbol{v}, q) \quad \forall\, (\boldsymbol{v}, q) \in \boldsymbol{V}_h \times Q_h, \tag{1.3}$$

where the bilinear form $\boldsymbol{B}^{BV}$ and linear form $\boldsymbol{F}^{BV}$ are defined as

$$\begin{aligned} \boldsymbol{B}^{BV}((\boldsymbol{u}, p), (\boldsymbol{v}, q)) &= \sigma(\boldsymbol{u}, \boldsymbol{v}) + \nu(\nabla\boldsymbol{u}, \nabla\boldsymbol{v}) - (p, \nabla\cdot\boldsymbol{v}) + (q, \nabla\cdot\boldsymbol{u}) \\ &\quad - \sum_{K\in\mathcal{T}_h} \tau_K(\sigma\boldsymbol{u} - \nu\Delta\boldsymbol{u} + \nabla p, \sigma\boldsymbol{v} - \nu\Delta\boldsymbol{v} - \nabla q)_{0,K}, \qquad (1.4) \\ \boldsymbol{F}^{BV}((\boldsymbol{v}, q)) &= (\boldsymbol{f}, \boldsymbol{v}) - \sum_{K\in\mathcal{T}_h} \tau_K(\boldsymbol{f}, \sigma\boldsymbol{v} - \nu\Delta\boldsymbol{v} - \nabla q)_{0,K}. \qquad (1.5) \end{aligned}$$

The factor τ_K is the so-called stabilization parameter, which is element-by-element defined as

$$\tau_K = \frac{h_K^2}{\sigma h_K^2 \xi(\lambda_K) + 4\nu/m_k}, \tag{1.6}$$

with

$$\xi(\lambda_K) = \max\{\lambda_K, 1\}, \quad \lambda_K = \frac{4\nu}{m_k \sigma h_K^2}, \quad m_k = \min\Big\{\frac{1}{3}, C_k\Big\},$$

and

$$\begin{cases} C_k h_K^2 \|\Delta v\|_{0,K}^2 \le \|\nabla v\|_{0,K}^2 \quad \forall\, v \in V_k, \\ V_k = \{v \in \mathcal{C}^0(\overline{\Omega}) : v|_K \in P_k(K), \forall\, K \in \mathcal{T}_h\}, \quad k \ge 1, \end{cases}$$

where $P_k(K)$ denotes the finite dimensional space of polynomials of degree not greater than k on the triangle $K \in \mathcal{T}_h$ and suitable values of the constant C_k in the local inverse inequality can be found in [28] for various orders k of finite elements. For example, if $k = 1$ then C_1 can be taken as any positive constant since $\|\Delta v\|_{0,K} = 0$, while if $k = 2$ then we take $C_2 = 1/42$.

The feature of this stabilization method is the subtraction of a term $\sum_{K\in\mathcal{T}_h} \tau_K(\sigma \boldsymbol{u}_h, \sigma \boldsymbol{v})_{0,K}$ from $\sigma(\boldsymbol{u}_h, \boldsymbol{v})_{0,\Omega}$, when compared with other stabilized methods (e.g., see [40]). This feature was also applied to advection-diffusion-reaction equations (e.g., [16], [23], and [30]). The following stability estimates and error bounds of the Barrenechea-Valentin FEM are proved in [3]:

- **Stability estimates (Lemma 3.1 and Lemma 4.2 in [3]):** *Given the bilinear form $\boldsymbol{B}^{BV}$ as above, we have the following stability estimates:*

  (i) There exists a constant $c_\Omega > 0$, depending only on Ω, such that

$$\boldsymbol{B}^{BV}((\boldsymbol{v}, q), (\boldsymbol{v}, q)) \ge c_\Omega \nu \|\boldsymbol{v}\|_1^2 + \sum_{K\in\mathcal{T}_h} \tau_K \|\nabla q\|_{0,K}^2 \quad \forall\, (\boldsymbol{v}, q) \in \boldsymbol{V}_h \times Q_h. \tag{1.7}$$

  (ii) There exists a constant $c(\sigma, \nu) > 0$, which depends on σ and ν, such that

$$\sup_{(\boldsymbol{v},q)\in \boldsymbol{V}_h\times Q_h} \frac{\boldsymbol{B}^{BV}((\boldsymbol{u}, p), (\boldsymbol{v}, q))}{(\|\boldsymbol{v}\|_1^2 + \|q\|_0^2)^{1/2}} \ge c(\sigma, \nu)\Big(\|\boldsymbol{u}\|_1^2 + \|p\|_0^2\Big)^{1/2} \quad \forall\, (\boldsymbol{u}, p) \in \boldsymbol{V}_h \times Q_h. \tag{1.8}$$

- **Error estimates (Theorem 3.1 and Theorem 4.1 in [3]):** *Assume that the solution $(\boldsymbol{u}, p)$ of problem (1.1) belongs to $(H^{k+1}(\Omega) \cap H_0^1(\Omega))^2 \times (H^{\ell+1}(\Omega) \cap L_0^2(\Omega))$. Let $(\boldsymbol{u}_h, p_h) \in \boldsymbol{V}_h \times Q_h$ be the finite element solution, where $\boldsymbol{V}_h = (V_k \cap H_0^1(\Omega))^2$ and $Q_h = V_\ell \cap L_0^2(\Omega)$. Then*

  (i) There exists $c(\sigma, \nu) > 0$, independent of h, but depending on σ and ν, such that

$$\begin{aligned} &\|\boldsymbol{u} - \boldsymbol{u}_h\|_1 + \Big(\sum_{K\in\mathcal{T}_h} \tau_K \|\nabla(p - p_h)\|_{0,K}^2\Big)^{1/2} \\ &\qquad \le c(\sigma, \nu) \frac{\max\{\sigma + 1, \nu + 1, \frac{1}{\sqrt{4\nu}}\}}{\min\{c_\Omega \nu, 1\}} \Big(h^k \|\boldsymbol{u}\|_{k+1} + h^{\ell+1} \|p\|_{\ell+1}\Big). \end{aligned} \tag{1.9}$$

  (ii) There exists $c(\sigma, \nu) > 0$, independent of h, but depending on σ and ν, such that

$$\|\boldsymbol{u} - \boldsymbol{u}_h\|_1 + \|p - p_h\|_0 \le c(\sigma, \nu) \max\Big\{\sigma, \nu + 1, \frac{1}{4\nu}\Big\} \Big(h^k \|\boldsymbol{u}\|_{k+1} + h^\ell \|p\|_\ell\Big). \tag{1.10}$$

Though above estimates are optimal, but it is not clear how the constants $c(\sigma, \nu)$ in these stability and error estimates vary with σ and ν. In the following sections, we are going to prove sharper stability and error estimates of the Barrenechea-Valentin stabilized FEM, revealing how the two constants σ and ν explicitly act on the stability and the error estimates.

For comparisons, we briefly state the main results of the error bounds obtained in this paper. Let $(\boldsymbol{u}_h, p_h) \in \boldsymbol{V}_h \times Q_h$ be the finite element solution pair and $(\boldsymbol{u}, p)$ the exact solution pair. Assuming quasi-uniform meshes with $h_K \ge ch$, we have the following error estimates:

- H^1 **semi-norm error bounds of velocity (cf. Theorem 3.1 below):**

$$\begin{aligned}\|\nabla(\boldsymbol{u}-\boldsymbol{u}_h)\|_0 &\leq c\Big(h^k|\boldsymbol{u}|_{k+1}+\frac{h^\ell}{\max\{\sigma h^2,4\nu/m\}}|p|_\ell\Big)\\ &\leq c\Big(h^k|\boldsymbol{u}|_{k+1}+\frac{h^{\ell-2}}{\sigma}|p|_\ell\Big), \qquad (1.11)\\ \|\nabla(\boldsymbol{u}-\boldsymbol{u}_h)\|_0 &\leq c\Big(h^k|\boldsymbol{u}|_{k+1}+\frac{h^{\ell+1}}{\max\{\sigma h^2,4\nu/m\}}|p|_{\ell+1}\Big)\\ &\leq c\Big(h^k|\boldsymbol{u}|_{k+1}+\frac{h^{\ell-1}}{\sigma}|p|_{\ell+1}\Big). \qquad (1.12)\end{aligned}$$

- L^2 **norm error bounds of velocity in convex domain (cf. Theorem 4.1 below):**

$$\begin{aligned}\|\boldsymbol{u}-\boldsymbol{u}_h\|_0 &\leq c\Big(h^{k+1}|\boldsymbol{u}|_{k+1}+\frac{h^{\ell+1}}{\max\{\sigma h^2,4\nu/m\}}|p|_\ell\Big)\\ &\leq c\Big(h^{k+1}|\boldsymbol{u}|_{k+1}+\frac{h^{\ell-1}}{\sigma}|p|_\ell\Big), \qquad (1.13)\\ \|\boldsymbol{u}-\boldsymbol{u}_h\|_0 &\leq c\Big(h^{k+1}|\boldsymbol{u}|_{k+1}+\frac{h^{\ell+2}}{\max\{\sigma h^2,4\nu/m\}}|p|_{\ell+1}\Big)\\ &\leq c\Big(h^{k+1}|\boldsymbol{u}|_{k+1}+\frac{h^{\ell}}{\sigma}|p|_{\ell+1}\Big). \qquad (1.14)\end{aligned}$$

- H^1 **semi-norm error bounds of pressure (cf. Theorem 3.2 below):**

$$\|\nabla(p_h-p)\|_0 \leq c\Big(h^{\ell-1}|p|_\ell+\nu h^{k-1}|\boldsymbol{u}|_{k+1}\Big), \qquad (1.15)$$

$$\|\nabla(p_h-p)\|_0 \leq c\Big(h^{\ell}|p|_{\ell+1}+\nu h^{k-1}|\boldsymbol{u}|_{k+1}\Big). \qquad (1.16)$$

We remark that all the constants c are independent of σ, ν, h, $\boldsymbol{u}$, and p.

The remainder of this paper is organized as follows. We derive sharp *a priori* stability estimates in Section 2 and error estimates in Section 3. In Section 4, we give the L^2 error estimates of the velocity in convex polygonal domains. We consider the practical values among ν, σ and h and then derive some improved error estimates in Section 5. Some numerical experiments are reported in Section 6. A brief summary and conclusion are given in Section 7.

2. Sharper a Priori Stability Estimates

Let $\boldsymbol{V}_h$ and Q_h be the continuous piecewise finite element spaces for velocity and pressure, respectively, defined as follows:

$$\begin{aligned}\boldsymbol{V}_h &= (V_k\cap H_0^1(\Omega))^d, \quad Q_h = V_\ell\cap L_0^2(\Omega),\\ V_k &= \{v\in\mathcal{C}^0(\overline{\Omega}): v|_K\in P_k(K), \forall\, K\in\mathcal{T}_h\}, \quad k,\ell\geq 1,\end{aligned} \qquad (2.1)$$

where $P_k(K)$ denotes the finite dimensional space of polynomials of degree not greater than k on the triangle or tetrahedron $K\in\mathcal{T}_h$, see [13]. To state the finite element problem, we first define

$$\begin{aligned} \boldsymbol{B}((\boldsymbol{u},p),(\boldsymbol{v},q)) &= \sigma(\boldsymbol{u},\boldsymbol{v}) + \nu(\nabla \boldsymbol{u},\nabla \boldsymbol{v}) - (p,\nabla\cdot\boldsymbol{v}) - (q,\nabla\cdot\boldsymbol{u}) \\ &\quad - \sum_{K\in\mathcal{T}_h} \tau_K(\sigma\boldsymbol{u} - \nu\Delta\boldsymbol{u} + \nabla p, \sigma\boldsymbol{v} - \nu\Delta\boldsymbol{v} + \nabla q)_{0,K}, \end{aligned} \tag{2.2}$$

$$\boldsymbol{F}(\boldsymbol{v},q) = (\boldsymbol{f},\boldsymbol{v}) - \sum_{K\in\mathcal{T}_h} \tau_K(\boldsymbol{f}, \sigma\boldsymbol{v} - \nu\Delta\boldsymbol{v} + \nabla q)_{0,K}, \tag{2.3}$$

$$\tau_K = \frac{h_K^2}{\sigma h_K^2 \xi(\lambda_K) + 4\nu/m_k}, \tag{2.4}$$

$$\xi(\lambda_K) = \max\{\lambda_K, 1\}, \quad \lambda_K = \frac{4\nu}{m_k \sigma h_K^2}, \tag{2.5}$$

with $m_1 = 1/3$ for linear elements on triangles ($d = 2$) or tetrahedra ($d = 3$), and otherwise, m_k is taken as any positive number satisfying

$$0 < m_k < 4\gamma C_k, \tag{2.6}$$

where γ is a given number with $0 < \gamma < 2 - \sqrt{3}$ and $C_k > 0$ is a given constant satisfying

$$\begin{cases} C_k h_K^2 \|\Delta v\|_{0,K}^2 \le \|\nabla v\|_{0,K}^2 \quad \forall\, v \in V_k, \quad \text{if } \Delta v \neq 0 \text{ on } K, \\ C_k > \dfrac{1}{12\gamma}, \quad \text{if } \Delta v = 0 \text{ on } K. \end{cases} \tag{2.7}$$

The first inequality in (2.7) is a classical local inverse estimate for finite dimensional functions. As tabulated in [28], the constant C_k which may differ from element to element depends only on the ratio of h_K/ρ_K and on the integer k of V_k. Under the shape-regular assumption, however, all C_k can be independent of h and K. We therefore always assume that C_k depends only on the shape-regularity constant α and the integer k of V_k. Note that only for linear elements on triangles (or tetrahedra for $d = 3$) we generally have $\Delta v = 0$. In that case, the constant C_1 can be any positive constant and we take $m_1 = 1/3$. However, for a general purpose, we put $C_1 > 1/(12\gamma)$ with a given $0 < \gamma < 2 - \sqrt{3}$, according to our analysis later on (see Proposition 2.1 and Theorem 2.1). The choice $m_1 = 1/3$ is well-known for linear elements on triangles or tetrahedra in the literature of stabilized methods, which may come from a multiscale-enrichment stabilized approach, e.g., see [1]. Also, note that the choice of m_k is more flexible here, with $m_k < 4\gamma C_k$ for any given $0 < \gamma < 2 - \sqrt{3}$. One may always choose a given value for γ, although any value of γ in the interval $(0, 2 - \sqrt{3})$ works. The well-known choice for m_k in the literature of stabilized methods is $0 < m_k \le C_k$ (see, e.g., [3] and [23]). This latter choice is also valid in our analysis, with a value for γ satisfying $1/4 < \gamma < 2 - \sqrt{3}$. To simplify the notations, in the rest of this paper, we shall exclusively put the following notations

$$\xi := \xi(\lambda_K), \quad m := m_k, \quad C := C_k.$$

The stabilized finite element problem we shall consider in this paper is to *find* $(\boldsymbol{u}_h, p_h) \in \boldsymbol{V}_h \times Q_h$ *such that*

$$\boldsymbol{B}((\boldsymbol{u}_h, p_h), (\boldsymbol{v}, q)) = \boldsymbol{F}(\boldsymbol{v}, q) \quad \forall\, (\boldsymbol{v}, q) \in \boldsymbol{V}_h \times Q_h. \tag{2.8}$$

The bilinear form $\boldsymbol{B}$ given in (2.2) is symmetric, slightly different from $\boldsymbol{B}^{BV}$ in (1.4). Accordingly, to keep the consistency property, we use a different linear form $\boldsymbol{F}$ given in (2.3). The reason why we would rather consider a symmetric method is that a symmetric linear system resulting from the finite element method would be more feasible for iterative solutions. Throughout this paper, we still call (2.1)-(2.8) the Barrenechea-Valentin stabilized FEM.

In the sequel, we shall investigate the stability of the finite element problem (2.8). For that goal, we first show a proposition that will be used later on in the analysis.

Proposition 2.1. *Let $0 < \gamma < 2 - \sqrt{3}$ and $0 < m < 4\gamma C$. Then for all $K \in \mathcal{T}_h$, we have*

$$\frac{1}{\gamma} \times \frac{\gamma\left(\sigma h_K^2 \xi + \nu(4/m - C^{-1})\right)\left(\sigma h_K^2(\xi - 1) + 4\nu/m\right) - \sigma \nu h_K^2 C^{-1}}{\left(\sigma h_K^2 \xi + 4\nu/m\right)\left(\sigma h_K^2(\xi - 1) + 4\nu/m\right)}$$
$$\geq \frac{4\gamma\xi - mC^{-1} + \gamma(\xi - 1)(4 - mC^{-1})}{4(2\xi - 1)} \geq \frac{4\gamma - mC^{-1}}{8} > 0. \tag{2.9}$$

Proof. The last inequality in (2.9) is obvious, because of $0 < m < 4\gamma C$. We next show the first and the second inequalities in (2.9). For convenience, letting $h := h_K$, we have

$$\frac{1}{\gamma} \times \frac{\gamma\left(\sigma h^2 \xi + \nu(4/m - C^{-1})\right)\left(\sigma h^2(\xi - 1) + 4\nu/m\right) - \sigma \nu h^2 C^{-1}}{\Big(\sigma h^2 \xi + 4\nu/m\Big)\Big(\sigma h^2(\xi - 1) + 4\nu/m\Big)}$$
$$= \frac{m\sigma^2 h^4 \xi(\xi - 1) + \sigma\nu h^2\Big(4\gamma\xi - mC^{-1} + \gamma(\xi - 1)(4 - mC^{-1})\Big)\gamma^{-1} + (4 - mC^{-1})4\nu^2/m}{m\sigma^2 h^4 \xi(\xi - 1) + 4\sigma\nu h^2(2\xi - 1) + 16\nu^2/m}$$
$$= \frac{4\gamma\xi - mC^{-1} + \gamma(\xi - 1)(4 - mC^{-1})}{4(2\xi - 1)}$$
$$\times \frac{4\sigma\nu h^2\gamma^{-1} + \dfrac{4m\sigma^2 h^4 \xi(\xi - 1)}{4\gamma\xi - mC^{-1} + \gamma(\xi - 1)(4 - mC^{-1})} + \dfrac{(16\nu^2/m)(4 - mC^{-1})}{4\gamma\xi - mC^{-1} + \gamma(\xi - 1)(4 - mC^{-1})}}{4\sigma\nu h^2 + \dfrac{m\sigma^2 h^4 \xi(\xi - 1)}{2\xi - 1} + \dfrac{16\nu^2/m}{2\xi - 1}}$$
$$:= T_1 \times T_2.$$

Since $\gamma^{-1} > 1$, if there hold the following two inequalities (2.10) and (2.11),

$$\frac{4}{4\gamma\xi - mC^{-1} + \gamma(\xi - 1)(4 - mC^{-1})} \geq \frac{1}{2\xi - 1} \tag{2.10}$$

and

$$\frac{4 - mC^{-1}}{4\gamma\xi - mC^{-1} + \gamma(\xi - 1)(4 - mC^{-1})} \geq \frac{1}{2\xi - 1}, \tag{2.11}$$

then we have $T_2 \geq 1$. That is to say, the first inequality in (2.9) holds, provided we have (2.10) and (2.11). Now we are going to prove (2.10) and (2.11). From the obvious facts that $0 < \gamma < 2 - \sqrt{3}$ and $\xi \geq 1$, the inequality (2.10) easily follows. Regarding (2.11), we respectively consider the two cases $\xi = 1$ if $4\nu \leq m\sigma h^2$ and $\xi = \frac{4\nu}{m\sigma h^2}$ if $4\nu > m\sigma h^2$. In the case $\xi = 1$, we have

$$\frac{4 - mC^{-1}}{4\gamma\xi - mC^{-1} + \gamma(\xi - 1)(4 - mC^{-1})} = \frac{4 - mC^{-1}}{4\gamma - mC^{-1}} \geq 1 = \frac{1}{2\xi - 1}.$$

In the case $\xi = \frac{4\nu}{m\sigma h^2}$ with $4\nu > m\sigma h^2$, to have (2.11), by inserting $\xi = \frac{4\nu}{m\sigma h^2}$, we find that (2.11) holds if

$$m\sigma h^2 \leq \frac{32\nu(1 - \gamma) - 4mC^{-1}\nu(2 - \gamma)}{4(1 - \gamma) - mC^{-1}(2 - \gamma)},$$

where $0 < \gamma < 2 - \sqrt{3}$ is chosen to ensure positive numerator and denominator in the above for all $0 < m < 4\gamma C$. But, $m\sigma h^2 < 4\nu$, it suffices to require

$$4\nu \leq \frac{32\nu(1-\gamma) - 4mC^{-1}\nu(2-\gamma)}{4(1-\gamma) - mC^{-1}(2-\gamma)}.$$

This inequality holds true indeed from a simple manipulation. Consequently, (2.11) is proven.

Next, we show the second inequality in (2.9). We consider the two choices, $\xi = 1$ and $\xi = \frac{4\nu}{m\sigma h^2}$ with $m\sigma h^2 < 4\nu$. If $\xi = 1$ we have

$$T_1 := \frac{4\gamma\xi - mC^{-1} + \gamma(\xi - 1)(4 - mC^{-1})}{4(2\xi - 1)} = \frac{4\gamma - mC^{-1}}{4}.$$

If $\xi = \frac{4\nu}{m\sigma h^2}$, inserting this ξ and using $m\sigma h^2 < 4\nu$, we have

$$\begin{aligned} T_1 &= \frac{32\nu\gamma - \big(4\gamma + (1-\gamma)mC^{-1}\big)m\sigma h^2 - 4\nu\gamma mC^{-1}}{4(8\nu - m\sigma h^2)} \\ &\geq \frac{32\nu\gamma - \big(4\gamma + (1-\gamma)mC^{-1}\big)4\nu - 4\nu\gamma mC^{-1}}{32\nu} = \frac{4\gamma - mC^{-1}}{8}. \end{aligned}$$

Hence, whatever ξ is, there holds the second inequality in (2.9). The proof is completed. □

The result in Proposition 2.1 is obtained from a careful investigation of the two choices of ξ. Such a trick will be frequently used in the sequel, in order to establish the explicit dependence on σ and ν in the error estimates. For the sake of notations, we re-state the result of Proposition 2.1 in the following:

$$1 - \frac{\sigma\nu\tau_K^2}{\gamma(1-\sigma\tau_K)Ch_K^2} \geq \widetilde{C} := \frac{4\gamma C - m}{8C} > 0.$$

Such inequality is uniform in h_K, σ and ν. We are now in a position to give the stability results. To do so, with τ_K being given by (2.4), we first define some norms, which will be used for the establishment of the stability, as follows:

$$|\boldsymbol{v}|_{1,\nu}^2 := \nu\widetilde{C}\|\nabla \boldsymbol{v}\|_0^2, \tag{2.12}$$

$$|\boldsymbol{v}|_{0,h}^2 := (1-\gamma)\sigma \sum_{K\in\mathcal{T}_h} (1-\sigma\tau_K)\|\boldsymbol{v}\|_{0,K}^2, \tag{2.13}$$

$$|q|_{1,h}^2 := \sum_{K\in\mathcal{T}_h} \tau_K \|\nabla q\|_{0,K}^2, \tag{2.14}$$

$$\|(\boldsymbol{v}, q)\|_h^2 := |\boldsymbol{v}|_{1,\nu}^2 + |\boldsymbol{v}|_{0,h}^2 + |q|_{1,h}^2. \tag{2.15}$$

Here we define the mesh-dependent L^2 norm $|\cdot|_{0,h}$ for velocity that is helpful for us to derive the optimal L^2 error bound for velocity in this paper, even if we do not apply the Aubin-Nitsche duality argument which is only applicable when Ω is convex or smooth [13]. See Corollary 3.1 and (5.5) in Section 5.

We remark that, in this paper, we shall use the letter c (possibly carrying subscripts of numbers) to denote a generic positive constant, which may be different at different occurrences. If not indicated explicitly, such c, which may depend on Ω, the shape-regularity constant α of triangulations and the integers k and ℓ in the approximations, is always independent of h, σ, ν, $K \in \mathcal{T}_h$, and of all the functions introduced.

We state the first result of the stability.

Theorem 2.1. *Let $0 < \gamma < 2-\sqrt{3}$ and $0 < m < 4\gamma C$. Then for all $(\boldsymbol{v},q) \in \boldsymbol{V}_h \times Q_h$, we have*

$$\boldsymbol{B}((\boldsymbol{v},q),(\boldsymbol{v},-q)) \geq \|(\boldsymbol{v},q)\|_h^2.$$

Proof. From (2.2), we have

$$\begin{aligned}\boldsymbol{B}((\boldsymbol{v},q),(\boldsymbol{v},-q)) &= \sigma\|\boldsymbol{v}\|_0^2 + \nu\|\nabla\boldsymbol{v}\|_0^2 - \sum_{K\in\mathcal{T}_h}\tau_K(\sigma\boldsymbol{v}-\nu\Delta\boldsymbol{v},\sigma\boldsymbol{v}-\nu\Delta\boldsymbol{v})_{0,K} + \sum_{K\in\mathcal{T}_h}\tau_K\|\nabla q\|_{0,K}^2\\ &= \nu\|\nabla\boldsymbol{v}\|_0^2 + \sum_{K\in\mathcal{T}_h}\tau_K\|\nabla q\|_{0,K}^2 + \sigma\sum_{K\in\mathcal{T}_h}(1-\sigma\tau_K)\|\boldsymbol{v}\|_{0,K}^2\\ &\quad + \sum_{K\in\mathcal{T}_h}2\sigma\nu\tau_K(\boldsymbol{v},\Delta\boldsymbol{v})_{0,K} - \sum_{K\in\mathcal{T}_h}\nu^2\tau_K\|\Delta\boldsymbol{v}\|_{0,K}^2,\end{aligned}$$

where, from the Young's inequality $2ab \leq \epsilon a^2 + \epsilon^{-1}b^2$ for any $\epsilon > 0$, choosing $\epsilon = \gamma$, we have

$$\sum_{K\in\mathcal{T}_h}2\sigma\nu\tau_K(\boldsymbol{v},\Delta\boldsymbol{v})_{0,K} \geq -\gamma\sigma\sum_{K\in\mathcal{T}_h}(1-\sigma\tau_K)\|\boldsymbol{v}\|_{0,K}^2 - \frac{\sigma}{\gamma}\sum_{K\in\mathcal{T}_h}\frac{\nu^2\tau_K^2}{1-\sigma\tau_K}\|\Delta\boldsymbol{v}\|_{0,K}^2,$$

and, from the local inverse estimate $Ch_K^2\|\Delta\boldsymbol{v}\|_{0,K}^2 \leq \|\nabla\boldsymbol{v}\|_{0,K}^2$ as given in (2.7), we have

$$\begin{aligned}\boldsymbol{B}((\boldsymbol{v},q),(\boldsymbol{v},-q)) \geq\ & \nu\sum_{K\in\mathcal{T}_h}\Big(1-\frac{\sigma\nu\tau_K^2}{\gamma(1-\sigma\tau_K)Ch_K^2}\Big)\|\nabla\boldsymbol{v}\|_{0,K}^2\\ & +(1-\gamma)\sigma\sum_{K\in\mathcal{T}_h}(1-\sigma\tau_K)\|\boldsymbol{v}\|_{0,K}^2 + \sum_{K\in\mathcal{T}_h}\tau_K\|\nabla q\|_{0,K}^2.\end{aligned}$$

Applying Proposition 2.1 and according to (2.12), (2.13), (2.14), (2.15), we obtain the desired stability. □

Theorem 2.1 provides a stability in L^2 norm for the pressure. In fact, considering the two choices $\xi = 1$, with $4\nu \leq m\sigma h_K^2$, and $\xi = \frac{4\nu}{m\sigma h_K^2}$, with $4\nu > m\sigma h_K^2$, from the Poincaré inequality (e.g., see [25])

$$\|q\|_0 \leq c\|\nabla q\|_0 \quad \forall\, q \in H^1(\Omega)\cap L_0^2(\Omega), \tag{2.16}$$

we have

$$|q|_{1,h}^2 \geq \min\Big\{\frac{1}{2\sigma},\ \min_{K\in\mathcal{T}_h}\frac{h_K^2}{8\nu/m}\Big\}\|q\|_0^2. \tag{2.17}$$

Since the numerical difficulties are often due to $4\nu \leq m\sigma h_K^2$, we can see that (2.17) already provides a discrete but *h-independent* stability in L^2 norm for the pressure. In other words, if $4\nu \leq m\sigma h_K^2$ for all $K \in \mathcal{T}_h$, from (2.17) we have

$$|q|_{1,h}^2 \geq \frac{1}{2\sigma}\|q\|_0^2. \tag{2.18}$$

In what follows, we shall establish a second stability result, where an *h-independent* L^2 norm is used for the pressure, regardless of the values of σ, ν and h_K. For that goal, we first recall a lemma.

Lemma 2.1. *For all $p \in Q_h$, there exists function $\boldsymbol{w} \in \boldsymbol{V}_h$ such that*

$$(\nabla\cdot\boldsymbol{w},p) \geq c_1\|p\|_0^2 - c_2(\sigma+\nu)|p|_{1,h}^2, \quad \|\boldsymbol{w}\|_1 \leq c_3\|p\|_0.$$

Proof. This lemma follows from Lemma 4.1 in [3]. □

We then define a norm with an L^2 norm for the pressure as follows:

$$|||(\boldsymbol{u},p)|||_h^2 = \|(\boldsymbol{u},p)\|_h^2 + (\sigma+\nu)^{-1}\|p\|_0^2, \tag{2.19}$$

where $\|(\boldsymbol{u},p)\|_h$ is given by (2.15). We have introduced a $(\sigma+\nu)$-weighted L^2 norm for the pressure, i.e., $\sqrt{(\sigma+\nu)^{-1}}\|\cdot\|_0$ (which is not presented in [3]). We shall use this norm to derive the L^2 norm error bound for the pressure. On the other hand, $\nu \le \sigma$ generally, so we have $1/(\sigma+\nu) \ge 1/(2\sigma)$, and the norm $\sqrt{(\sigma+\nu)^{-1}}\|\cdot\|_0$ amounts to $\sqrt{1/(2\sigma)}\|\cdot\|_0$, see also (2.18).

Now the second result of the stability is stated in the following. We have explicitly worked out how the stability constants in Theorem 2.1 and Theorem 2.2 depend on ν, σ and h_K. In fact, the dependence is explicitly reflected in the norms used.

Theorem 2.2. *Let $0 < \gamma < 2-\sqrt{3}$ and $0 < m < 4\gamma C$. Then we have*

$$\sup_{(\boldsymbol{v},q)\in \boldsymbol{V}_h\times Q_h} \frac{\boldsymbol{B}((\boldsymbol{u},p),(\boldsymbol{v},q))}{|||(\boldsymbol{v},q)|||_h} \ge c|||(\boldsymbol{u},p)|||_h \quad \forall\,(\boldsymbol{u},p)\in \boldsymbol{V}_h\times Q_h.$$

Proof. For any given $p \in Q_h$, from Lemma 2.1, there exists a $\boldsymbol{w}\in \boldsymbol{V}_h$ such that

$$(\nabla\cdot\boldsymbol{w},p) \ge c_1\|p\|_0^2 - c_2(\sigma+\nu)|p|_{1,h}^2, \quad \|\boldsymbol{w}\|_1 \le c_3\|p\|_0.$$

With this $\boldsymbol{w}$, we have

$$\begin{aligned}
\boldsymbol{B}((\boldsymbol{u},p),(-\boldsymbol{w},0)) &= -\sigma(\boldsymbol{u},\boldsymbol{w}) - \nu(\nabla\boldsymbol{u},\nabla\boldsymbol{w}) + (p,\nabla\cdot\boldsymbol{w}) \\
&\quad + \sum_{K\in\mathcal{T}_h}\tau_K(\sigma\boldsymbol{u}-\nu\Delta\boldsymbol{u}+\nabla p, \sigma\boldsymbol{w}-\nu\Delta\boldsymbol{w})_{0,K} \\
&= -\sigma\sum_{K\in\mathcal{T}_h}(1-\sigma\tau_K)(\boldsymbol{u},\boldsymbol{w})_{0,K} - \nu(\nabla\boldsymbol{u},\nabla\boldsymbol{w}) + (p,\nabla\cdot\boldsymbol{w}) \\
&\quad - \sum_{K\in\mathcal{T}_h}\tau_K\sigma\nu(\Delta\boldsymbol{u},\boldsymbol{w})_{0,K} - \sum_{K\in\mathcal{T}_h}\tau_K\sigma\nu(\boldsymbol{u},\Delta\boldsymbol{w})_{0,K} + \sum_{K\in\mathcal{T}_h}\tau_K\nu^2(\Delta\boldsymbol{u},\Delta\boldsymbol{w})_{0,K} \\
&\quad + \sum_{K\in\mathcal{T}_h}\tau_K\sigma(\nabla p,\boldsymbol{w})_{0,K} - \sum_{K\in\mathcal{T}_h}\tau_K\nu(\nabla p,\Delta\boldsymbol{w})_{0,K},
\end{aligned}$$

where the lower bound of the term $(p,\nabla\cdot\boldsymbol{w})$ is known, and the rest seven terms will be estimated one-by-one below. For this purpose, we first list some inequalities we shall use for all $K\in\mathcal{T}_h$ and for all $k\ge 1$. By considering the two choices $\xi = 1$ for $4\nu \le m\sigma h_K^2$ and $\xi = 4\nu/(m\sigma h_K^2)$ for $4\nu > m\sigma h_K^2$, we can show the following three inequalities:

$$\tau_K\sigma h_K^{-1}\sqrt{\nu}C^{-1/2} = \frac{\sigma h_K\sqrt{\nu}C^{-1/2}}{\sigma h_K^2\xi + 4\nu/m} \le \frac{\sqrt{m\sigma}C^{-1/2}}{2},$$

$$\frac{\tau_K^2\sigma\nu^2C^{-1}h_K^{-2}}{1-\sigma\tau_K} = \frac{h_K^2\sigma\nu^2C^{-1}}{(\sigma h_K^2\xi+4\nu/m)(\sigma h_K^2(\xi-1)+4\nu/m)} \le \frac{m\nu C^{-1}}{4},$$

$$\tau_K\nu^2C^{-1}h_K^{-2} = \frac{\nu^2C^{-1}}{\sigma h_K^2\xi+4\nu/m} \le \frac{mC^{-1}\nu}{4}.$$

In fact, to show the above first inequality, for example, when $\xi = 1$ for $4\nu \leq m\sigma h_K^2$, we have

$$\begin{aligned}\frac{\sigma h_K\sqrt{\nu}C^{-1/2}}{\sigma h_K^2\xi + 4\nu/m} &= \frac{\sigma h_K\sqrt{\nu}C^{-1/2}}{\sigma h_K^2 + 4\nu/m} \leq \frac{\sigma h_K\sqrt{m\sigma h_K^2/4}C^{-1/2}}{\sigma h_K^2 + 4\nu/m} \\ &= \frac{\sigma h_K^2\sqrt{m\sigma}C^{-1/2}}{2(\sigma h_K^2 + 4\nu/m)} \leq \frac{\sigma h_K^2\sqrt{m\sigma}C^{-1/2}}{2\sigma h_K^2} = \frac{\sqrt{m\sigma}C^{-1/2}}{2};\end{aligned}$$

when $\xi = 4\nu/(m\sigma h_K^2)$ for $4\nu > m\sigma h_K^2$, we have

$$\begin{aligned}\frac{\sigma h_K\sqrt{\nu}C^{-1/2}}{\sigma h_K^2\xi + 4\nu/m} &= \frac{\sigma h_K\sqrt{\nu}C^{-1/2}}{8\nu/m} = \frac{\sigma h_K m C^{-1/2}}{8\sqrt{\nu}} \\ &\leq \frac{\sigma h_K m C^{-1/2}}{8\sqrt{m\sigma h_K^2/4}} = \frac{\sqrt{m\sigma}C^{-1/2}}{4} < \frac{\sqrt{m\sigma}C^{-1/2}}{2}.\end{aligned}$$

Other inequalities can be similarly shown. In addition, since $\xi \geq 1$, the following two inequalities obviously hold:

$$\sigma\tau_K = \frac{\sigma h_K^2}{\sigma h_K^2\xi + 4\nu/m} \leq 1 \quad \text{and} \quad 0 < 1 - \sigma\tau_K = \frac{\sigma h_K^2(\xi - 1) + 4\nu/m}{\sigma h_K^2\xi + 4\nu/m} \leq 1.$$

We shall also use the Young's inequality $ab \leq \frac{\epsilon}{2}a^2 + \frac{1}{2\epsilon}b^2$ for all $\epsilon > 0$.

Considering the first term, from the Cauchy-Schwarz inequality, the Young's inequality, the inequality $1 - \sigma\tau_K \leq 1$, and the norm (2.13), we have

$$\begin{aligned}&-\sigma\sum_{K\in\mathcal{T}_h}(1-\sigma\tau_K)(\boldsymbol{u},\boldsymbol{w})_{0,K} \geq -\sigma\sum_{K\in\mathcal{T}_h}(1-\sigma\tau_K)\|\boldsymbol{u}\|_{0,K}\|\boldsymbol{w}\|_{0,K} \\ &\geq -\frac{\epsilon\sigma}{2(1-\gamma)}\sum_{K\in\mathcal{T}_h}(1-\sigma\tau_K)\|\boldsymbol{w}\|_{0,K}^2 - \frac{1}{2\epsilon}(1-\gamma)\sigma\sum_{K\in\mathcal{T}_h}(1-\sigma\tau_K)\|\boldsymbol{u}\|_{0,K}^2 \\ &\geq -\frac{\epsilon\sigma}{2(1-\gamma)}\|\boldsymbol{w}\|_0^2 - \frac{1}{2\epsilon}|\boldsymbol{u}|_{0,h}^2.\end{aligned}$$

Considering the second term, from the Cauchy-Schwarz inequality, the Young's inequality and the norm (2.12), we have

$$-\nu(\nabla\boldsymbol{u},\nabla\boldsymbol{w}) \geq -\nu\|\nabla\boldsymbol{u}\|_0\|\nabla\boldsymbol{w}\|_0 \geq -\frac{\epsilon\nu}{2\tilde{C}}\|\nabla\boldsymbol{w}\|_0^2 - \frac{1}{2\epsilon}|\boldsymbol{u}|_{1,\nu}^2.$$

Considering the third term, from the Cauchy-Schwarz inequality, the local inverse estimate $Ch_K^2\|\Delta\boldsymbol{v}\|_{0,K}^2 \leq \|\nabla\boldsymbol{v}\|_{0,K}^2$, the inequality $\tau_K\sigma h_K^{-1}\sqrt{\nu}C^{-1/2} \leq \sqrt{m\sigma}C^{-1/2}/2$, the norm (2.12), and the Young's inequality, we have

$$\begin{aligned}-\sum_{K\in\mathcal{T}_h}\tau_K\sigma\nu(\Delta\boldsymbol{u},\boldsymbol{w})_{0,K} &\geq -\sum_{K\in\mathcal{T}_h}\tau_K\sigma\nu\|\Delta\boldsymbol{u}\|_{0,K}\|\boldsymbol{w}\|_{0,K} \\ &\geq -\sum_{K\in\mathcal{T}_h}\tau_K\sigma h_K^{-1}\nu C^{-1/2}\|\nabla\boldsymbol{u}\|_{0,K}\|\boldsymbol{w}\|_{0,K} \\ &\geq -\frac{\sqrt{\nu}\sqrt{m\sigma}C^{-1/2}}{2}\|\nabla\boldsymbol{u}\|_0\|\boldsymbol{w}\|_0 \\ &\geq -\frac{\epsilon m\sigma}{8C\tilde{C}}\|\boldsymbol{w}\|_0^2 - \frac{1}{2\epsilon}|\boldsymbol{u}|_{1,\nu}^2.\end{aligned}$$

Considering the fourth term, from the Cauchy-Schwarz inequality, the local inverse estimate $Ch_K^2\|\Delta v\|_{0,K}^2 \leq \|\nabla v\|_{0,K}^2$, the norm (2.13), the inequality $\tau_K^2\sigma\nu^2C^{-1}h_K^{-2}/(1-\sigma\tau_K) \leq m\nu C^{-1}/4$, and the Young's inequality, we have

$$\begin{aligned}
-\sum_{K\in\mathcal{T}_h}\tau_K\sigma\nu(\boldsymbol{u},\Delta\boldsymbol{w})_{0,K} &\geq -\sum_{K\in\mathcal{T}_h}\tau_K\sigma\nu\|\boldsymbol{u}\|_{0,K}\|\Delta\boldsymbol{w}\|_{0,K}\\
&\geq -\sum_{K\in\mathcal{T}_h}\tau_K\sigma\nu C^{-1/2}h_K^{-1}\|\nabla\boldsymbol{w}\|_{0,K}\|\boldsymbol{u}\|_{0,K}\\
&\geq -\Big(\sum_{K\in\mathcal{T}_h}\frac{\tau_K^2\sigma\nu^2C^{-1}h_K^{-2}}{1-\sigma\tau_K}\|\nabla\boldsymbol{w}\|_{0,K}^2\Big)^{1/2}\frac{1}{\sqrt{1-\gamma}}|\boldsymbol{u}|_{0,h}\\
&\geq -\frac{\epsilon m\nu}{8C(1-\gamma)}\|\nabla\boldsymbol{w}\|_0^2-\frac{1}{2\epsilon}|\boldsymbol{u}|_{0,h}^2.
\end{aligned}$$

Considering the fifth term, from the Cauchy-Schwarz inequality, the local inverse estimate $Ch_K^2\|\Delta v\|_{0,K}^2 \leq \|\nabla v\|_{0,K}^2$, the norm (2.12), the inequality $\tau_K\nu^2C^{-1}h_K^{-2} \leq m\nu C^{-1}/4$, and the Young's inequality, we have

$$\begin{aligned}
\sum_{K\in\mathcal{T}_h}\tau_K\nu^2(\Delta\boldsymbol{u},\Delta\boldsymbol{w})_{0,K} &\geq -\sum_{K\in\mathcal{T}_h}\tau_K\nu^2C^{-1}h_K^{-2}\|\nabla\boldsymbol{w}\|_{0,K}\|\nabla\boldsymbol{u}\|_{0,K}\\
&\geq -\frac{m\nu C^{-1}}{4}\|\nabla\boldsymbol{w}\|_0\|\nabla\boldsymbol{u}\|_0 = -\frac{m\sqrt{\nu}}{4C\widetilde{C}^{1/2}}\|\nabla\boldsymbol{w}\|_0|\boldsymbol{u}|_{1,\nu}\\
&\geq -\frac{\epsilon m^2\nu}{32C^2\widetilde{C}}\|\nabla\boldsymbol{w}\|_0^2-\frac{1}{2\epsilon}|\boldsymbol{u}|_{1,\nu}^2.
\end{aligned}$$

Considering the sixth term, from the Cauchy-Schwarz inequality, the inequality $\sigma\tau_K \leq 1$, the norm (2.14), and the Young's inequality, we have

$$\begin{aligned}
\sum_{K\in\mathcal{T}_h}\tau_K\sigma(\nabla p,\boldsymbol{w})_{0,K} &\geq \sum_{K\in\mathcal{T}_h}\tau_K\sigma\|\nabla p\|_{0,K}\|\boldsymbol{w}\|_{0,K}\\
&\geq -\Big(\sum_{K\in\mathcal{T}_h}\tau_K\sigma^2\|\boldsymbol{w}\|_{0,K}^2\Big)^{1/2}|p|_{1,h}\\
&\geq -\frac{\epsilon\sigma}{2}\|\boldsymbol{w}\|_0^2-\frac{1}{2\epsilon}|p|_{1,h}^2.
\end{aligned}$$

Considering the seventh term, from the Cauchy-Schwarz inequality, the local inverse estimate $Ch_K^2\|\Delta v\|_{0,K}^2 \leq \|\nabla v\|_{0,K}^2$, the norm (2.14), the inequality $\tau_K\nu^2C^{-1}h_K^{-2} \leq m\nu C^{-1}/4$, and the Young's inequality, we have

$$\begin{aligned}
-\sum_{K\in\mathcal{T}_h}\tau_K\nu(\nabla p,\Delta\boldsymbol{w})_{0,K} &\geq -\sum_{K\in\mathcal{T}_h}\tau_K\nu\|\nabla p\|_{0,K}\|\Delta\boldsymbol{w}\|_{0,K}\\
&\geq -\sum_{K\in\mathcal{T}_h}\tau_K\nu C^{-1/2}h_K^{-1}\|\nabla p\|_{0,K}\|\nabla\boldsymbol{w}\|_{0,K}\\
&\geq -\Big(\sum_{K\in\mathcal{T}_h}\tau_K\nu^2C^{-1}h_K^{-2}\|\nabla\boldsymbol{w}\|_{0,K}^2\Big)^{1/2}|p|_{1,h}\\
&\geq -\frac{\epsilon m\nu}{8C}\|\nabla\boldsymbol{w}\|_0^2-\frac{1}{2\epsilon}|p|_{1,h}^2.
\end{aligned}$$

Combining all the above and the Friedrichs-Poincaré inequality (e.g., see [25])

$$\|\boldsymbol{z}\|_0 \leq c_4\|\nabla\boldsymbol{z}\|_0 \quad \forall\, \boldsymbol{z}\in(H_0^1(\Omega))^d, \tag{2.20}$$

we have

$$\begin{aligned}&\boldsymbol{B}((\boldsymbol{u},p),(-\boldsymbol{w},0))\\&\geq \left\{c_1-\epsilon\Big(\frac{c_4^2\sigma}{2(1-\gamma)}+\frac{\nu}{2\widetilde{C}}+\frac{m\sigma c_4^2}{8C\widetilde{C}}+\frac{m\nu}{8C(1-\gamma)}+\frac{m^2\nu}{32C^2\widetilde{C}}+\frac{c_4^2\sigma}{2}+\frac{m\nu}{8C}\Big)\right\}\|p\|_0^2\\&\quad-\frac{1}{2\epsilon}(2|\boldsymbol{u}|_{0,h}^2+2|p|_{1,h}^2+3|\boldsymbol{u}|_{1,\nu}^2)-c_2(\sigma+\nu)|p|_{1,h}^2,\end{aligned}$$

where

$$\begin{aligned}&\frac{c_4^2\sigma}{2(1-\gamma)}+\frac{\nu}{2\widetilde{C}}+\frac{m\sigma c_4^2}{8C\widetilde{C}}+\frac{m\nu}{8C(1-\gamma)}+\frac{m^2\nu}{32C^2\widetilde{C}}+\frac{c_4^2\sigma}{2}+\frac{m\nu}{8C}\\&\leq(\sigma+\nu)\Big(\frac{c_4^2}{2(1-\gamma)}+\frac{1}{2\widetilde{C}}+\frac{mc_4^2}{8C\widetilde{C}}+\frac{m}{8C(1-\gamma)}+\frac{m^2}{32C^2\widetilde{C}}+\frac{c_4^2}{2}+\frac{m}{8C}\Big)\\&:=c_5(\sigma+\nu).\end{aligned}$$

Now choosing

$$\epsilon=\frac{c_1}{2c_5(\sigma+\nu)}$$

and $c_6:=3c_5/c_1+c_2$, we obtain

$$\boldsymbol{B}((\boldsymbol{u},p),(-\boldsymbol{w},0))\geq\frac{c_1}{2}\|p\|_0^2-c_6(\sigma+\nu)\|(\boldsymbol{u},p)\|_h^2.$$

Choosing

$$(\boldsymbol{v},q)=(\boldsymbol{u}-\delta\boldsymbol{w},-p),\quad \delta=\frac{1}{2c_6(\sigma+\nu)},$$

and putting $c_7:=\min(1/2,c_1/(4c_6))$, we have

$$\begin{aligned}\boldsymbol{B}((\boldsymbol{u},p),(\boldsymbol{v},q))&=\delta\boldsymbol{B}((\boldsymbol{u},p),(-\boldsymbol{w},0))+\boldsymbol{B}((\boldsymbol{u},p),(\boldsymbol{u},-p))\\&\geq\delta c_1/2\|p\|_0^2+\big(1-\delta c_6(\sigma+\nu)\big)\|(\boldsymbol{u},p)\|_h^2\\&=\frac{c_1}{4c_6(\sigma+\nu)}\|p\|_0^2+\frac{1}{2}\|(\boldsymbol{u},p)\|_h^2\\&\geq c_7|||(\boldsymbol{u},p)|||_h^2.\end{aligned}$$

In addition, since

$$|\boldsymbol{w}|_{0,h}\leq\sqrt{\sigma}\|\boldsymbol{w}\|_0,\quad |\boldsymbol{w}|_{1,\nu}=\sqrt{\nu\widetilde{C}}\|\nabla\boldsymbol{w}\|_0,$$

it can be verified that

$$|||(\mathbf{v},q)|||_h=|||(\mathbf{u}-\delta\mathbf{w},-p)|||_h\leq c_8|||(\mathbf{u},p)|||_h.$$

Finally, we obtain the desired stability estimate, with the constant $c:=c_7/c_8$. This completes the proof. □

3. Sharper a Priori Error Estimates

With the stability established in the previous section, we now can analyze the error estimates. We first recall the classical finite element interpolation properties (see [13] and [25]):

$$k\geq1,\quad 2\leq t\leq k+1,\quad \ell\geq1,\quad 1\leq s\leq\ell+1,$$

$$\|\boldsymbol{u} - \boldsymbol{I}_h\boldsymbol{u}\|_{0,K} \leq c h_K^t |\boldsymbol{u}|_{t,K}, \tag{3.1}$$

$$\|\nabla(\boldsymbol{u} - \boldsymbol{I}_h\boldsymbol{u})\|_{0,K} \leq c h_K^{t-1} |\boldsymbol{u}|_{t,K}, \tag{3.2}$$

$$\|\Delta(\boldsymbol{u} - \boldsymbol{I}_h\boldsymbol{u})\|_{0,K} \leq c h_K^{k-1} |\boldsymbol{u}|_{k+1,K}, \tag{3.3}$$

$$\|p - J_h p\|_0 \leq c h^s \|p\|_s, \tag{3.4}$$

$$\|\nabla(p - J_h p)\|_{0,K} \leq c h_K^{s-1} \|p\|_{s,D_K}, \tag{3.5}$$

where D_K denotes the union of all support sets of basis functions in $P_\ell(K)$ on K, and $\boldsymbol{I}_h$ is the standard nodal-based interpolation operator and J_h is the Clément interpolation operator, with an obvious modification so that $\int_\Omega J_h p = 0$, i.e, $J_h p \in L_0^2(\Omega)$.

For a given $p \in H^1(\Omega) \cap L_0^2(\Omega)$, we define a finite element projection $\widetilde{p} \in Q_h$, such that

$$\sum_{K \in \mathcal{T}_h} \tau_K (\nabla \widetilde{p}, \nabla q)_{0,K} = \sum_{K \in \mathcal{T}_h} \tau_K (\nabla p, \nabla q)_{0,K} \quad \forall\, q \in Q_h. \tag{3.6}$$

The unique existence of such a $\widetilde{p} \in Q_h$ is because that $|\cdot|_{1,h}$ is a norm over Q_h. Taking

$$q = \widetilde{p} - J_h p,$$

we have

$$|q|_{1,h}^2 = \sum_{K \in \mathcal{T}_h} \tau_K (\nabla(\widetilde{p} - J_h p), \nabla q)_{0,K} = \sum_{K \in \mathcal{T}_h} \tau_K (\nabla(p - J_h p), \nabla q)_{0,K} \leq |p - J_h p|_{1,h} |q|_{1,h},$$

that is,

$$|\widetilde{p} - J_h p|_{1,h} \leq |p - J_h p|_{1,h},$$

and by the triangle inequality we have

$$|p - \widetilde{p}|_{1,h} \leq 2|p - J_h p|_{1,h}. \tag{3.7}$$

Remark 3.1. *Due to the Poincaré inequality (2.16), we can obtain the error estimates for $\|p - \widetilde{p}\|_0$, with the same order in h as in the error estimates for $\|\nabla(p - \widetilde{p})\|_0$. On the other hand, since τ_K is element-dependent, it seems to be difficult if one can apply the classical Aubin-Nitsche duality argument to obtain a better estimate of $\|p - \widetilde{p}\|_0$. However, if τ_K is the same for all $K \in \mathcal{T}_h$, then $\widetilde{p}$ is the standard finite element projection [25], satisfying the classical result $\|p - \widetilde{p}\|_0 \leq ch\|\nabla(p - \widetilde{p})\|_0$ for a convex domain Ω.*

We remark that the stabilization method (2.8) is a consistent formulation, since (2.8) is satisfied when the finite element solution $(\boldsymbol{u}_h, p_h)$ is replaced by the exact solution $(\boldsymbol{u}, p)$ of problem (1.1). As a consequence, we have the following consistency or orthogonality property:

$$\boldsymbol{B}((\boldsymbol{u}, p) - (\boldsymbol{u}_h, p_h), (\boldsymbol{v}, q)) = 0 \quad \forall\, (\boldsymbol{v}, q) \in \boldsymbol{V}_h \times Q_h. \tag{3.8}$$

In Lemma 3.1 below, we obtain the error bounds between the finite element solutions and the finite element interpolations of the exact solutions, where the argument and the results are critical for all the analysis and results obtained in the sequel.

Lemma 3.1. *Let $(\boldsymbol{u}_h, p_h) \in \boldsymbol{V}_h \times Q_h$ denote the finite element solution pair to problem (2.8). Assume that the exact solution pair $(\boldsymbol{u}, p) \in (H^{k+1}(\Omega) \cap H_0^1(\Omega))^d \times (H^\ell(\Omega) \cap L_0^2(\Omega))$ for $k, \ell \geq 1$. Choosing $\widetilde{\boldsymbol{u}} = \boldsymbol{I}_h \boldsymbol{u} \in \boldsymbol{V}_h$ satisfying (3.1), (3.2) and (3.3) and $\widetilde{p} \in Q_h$ satisfying (3.6) and (3.7), where $J_h p$ satisfies (3.4) and (3.5), we have*

$$
\begin{aligned}
\|\nabla(\boldsymbol{u}_h - \widetilde{\boldsymbol{u}})\|_0 &\leq c\Big(h^k|\boldsymbol{u}|_{k+1} + \frac{h^{\ell-1}}{\sigma}\max_{K\in\mathcal{T}_h} h_K^{-1}|p|_\ell\Big),\\
|\boldsymbol{u}_h - \widetilde{\boldsymbol{u}}|_{0,h} &\leq c\sqrt{\nu}\Big(h^k|\boldsymbol{u}|_{k+1} + \frac{h^{\ell-1}}{\sigma}\max_{K\in\mathcal{T}_h} h_K^{-1}|p|_\ell\Big),\\
|p_h - \widetilde{p}|_{1,h} &\leq c\sqrt{\nu}\Big(h^k|\boldsymbol{u}|_{k+1} + \frac{h^{\ell-1}}{\sigma}\max_{K\in\mathcal{T}_h} h_K^{-1}|p|_\ell\Big),\\
\|p_h - \widetilde{p}\|_0 &\leq c\sqrt{(\sigma+\nu)\nu}\Big(h^k|\boldsymbol{u}|_{k+1} + \frac{h^{\ell-1}}{\sigma}\max_{K\in\mathcal{T}_h} h_K^{-1}|p|_\ell\Big),
\end{aligned}
$$

where $|\cdot|_{0,h}$ and $|\cdot|_{1,h}$ are given by (2.13) and (2.14), respectively.

Proof. Set $(\boldsymbol{w}, z) = (\boldsymbol{u}_h - \widetilde{\boldsymbol{u}}, p_h - \widetilde{p}) \in \mathbf{V}_h \times Q_h$, where $\widetilde{\boldsymbol{u}} = \boldsymbol{I}_h\boldsymbol{u}$. We have from the stability in Theorem 2.2 and the orthogonality property (3.8) that

$$
c|||(\boldsymbol{w}, z)|||_h \leq \sup_{(\boldsymbol{v},q)\in\boldsymbol{V}_h\times Q_h} \frac{\boldsymbol{B}((\boldsymbol{w},z),(\boldsymbol{v},q))}{|||(\boldsymbol{v},q)|||_h}, \tag{3.9}
$$

and

$$
\begin{aligned}
&\boldsymbol{B}((\boldsymbol{w},z),(\boldsymbol{v},q)) = \boldsymbol{B}((\boldsymbol{u}-\widetilde{\boldsymbol{u}}, p-\widetilde{p}),(\boldsymbol{v},q))\\
&= \sigma(\boldsymbol{u}-\widetilde{\boldsymbol{u}},\boldsymbol{v}) + \nu(\nabla(\boldsymbol{u}-\widetilde{\boldsymbol{u}}),\nabla\boldsymbol{v}) - (p-\widetilde{p},\nabla\cdot\boldsymbol{v}) - (q,\nabla\cdot(\boldsymbol{u}-\widetilde{\boldsymbol{u}}))\\
&\quad - \sum_{K\in\mathcal{T}_h}\tau_K(\sigma(\boldsymbol{u}-\widetilde{\boldsymbol{u}}) - \nu\Delta(\boldsymbol{u}-\widetilde{\boldsymbol{u}}) + \nabla(p-\widetilde{p}), \sigma\boldsymbol{v} - \nu\Delta\boldsymbol{v} + \nabla q)_{0,K}\\
&= \underbrace{\nu(\nabla(\boldsymbol{u}-\widetilde{\boldsymbol{u}}),\nabla\boldsymbol{v})}_{I_1} + \underbrace{\sigma(\boldsymbol{u}-\widetilde{\boldsymbol{u}},\boldsymbol{v}) - \sum_{K\in\mathcal{T}_h}\tau_K(\sigma(\boldsymbol{u}-\widetilde{\boldsymbol{u}}),\sigma\boldsymbol{v})_{0,K}}_{I_2}\\
&\quad \underbrace{-(p-\widetilde{p},\nabla\cdot\boldsymbol{v}) - \sum_{K\in\mathcal{T}_h}\tau_K(\nabla(p-\widetilde{p}),\sigma\boldsymbol{v})_{0,K}}_{I_3} \underbrace{-(q,\nabla\cdot(\boldsymbol{u}-\widetilde{\boldsymbol{u}})) - \sum_{K\in\mathcal{T}_h}\tau_K(\sigma(\boldsymbol{u}-\widetilde{\boldsymbol{u}}),\nabla q)_{0,K}}_{I_4}\\
&\quad \underbrace{-\sum_{K\in\mathcal{T}_h}\tau_K(\sigma(\boldsymbol{u}-\widetilde{\boldsymbol{u}}),-\nu\Delta\boldsymbol{v})_{0,K}}_{I_5} \underbrace{-\sum_{K\in\mathcal{T}_h}\tau_K(-\nu\Delta(\boldsymbol{u}-\widetilde{\boldsymbol{u}}),\sigma\boldsymbol{v})_{0,K}}_{I_6}\\
&\quad \underbrace{-\sum_{K\in\mathcal{T}_h}\tau_K(-\nu\Delta(\boldsymbol{u}-\widetilde{\boldsymbol{u}}),-\nu\Delta\boldsymbol{v})_{0,K}}_{I_7} \underbrace{-\sum_{K\in\mathcal{T}_h}\tau_K(-\nu\Delta(\boldsymbol{u}-\widetilde{\boldsymbol{u}}),\nabla q)_{0,K}}_{I_8}\\
&\quad \underbrace{-\sum_{K\in\mathcal{T}_h}\tau_K(\nabla(p-\widetilde{p}),-\nu\Delta\boldsymbol{v})_{0,K}}_{I_9} \underbrace{-\sum_{K\in\mathcal{T}_h}\tau_K(\nabla(p-\widetilde{p}),\nabla q)_{0,K}}_{I_{10}}.
\end{aligned}
$$

Below, we shall estimate the above terms $I_i, i = 1, 2, \cdots, 10$. First, according to the norm (2.12) and the interpolation estimate (3.2), we have

$$
I_1 \leq \sqrt{\nu\widetilde{C}}\|\nabla(\boldsymbol{u}-\widetilde{\boldsymbol{u}})\|_0|\boldsymbol{v}|_{1,\nu} \leq c\sqrt{\nu}h^k|\boldsymbol{u}|_{k+1}|\boldsymbol{v}|_{1,\nu}.
$$

According to the norm (2.13) and the interpolation estimate (3.1), we have

$$\begin{aligned} I_2 &= \sigma \sum_{K\in\mathcal{T}_h} (1-\sigma\tau_K)(\boldsymbol{u}-\widetilde{\boldsymbol{u}},\boldsymbol{v})_{0,K} \le c\Big(\sum_{K\in\mathcal{T}_h} \sigma(1-\sigma\tau_K)\|\boldsymbol{u}-\widetilde{\boldsymbol{u}}\|_{0,K}^2\Big)^{1/2}|\boldsymbol{v}|_{0,h} \\ &\le c\Big(\sum_{K\in\mathcal{T}_h} \sigma(1-\sigma\tau_K)h_K^{2(k+1)}|\boldsymbol{u}|_{k+1,K}^2\Big)^{1/2}|\boldsymbol{v}|_{0,h} \le c\sqrt{\nu}h^k|\boldsymbol{u}|_{k+1}|\boldsymbol{v}|_{0,h}, \end{aligned}$$

where we have used the estimate

$$\sigma h_K^2(1-\sigma\tau_K) \le 4\nu/m$$

which can be shown from the function $\xi(\cdot)$ with $\xi = 1$ if $4\nu \le m\sigma h_K^2$ and $\xi = \frac{4\nu}{m\sigma h_K^2}$ if $4\nu > m\sigma h_K^2$. In fact, since

$$\sigma h_K^2(1-\sigma\tau_K) = \sigma h_K^2 \frac{\sigma h_K^2(\xi-1)+4\nu/m}{\sigma h_K^2\xi+4\nu/m},$$

when $\xi = 1$ if $4\nu \le m\sigma h_K^2$, we have

$$\sigma h_K^2 \frac{\sigma h_K^2(\xi-1)+4\nu/m}{\sigma h_K^2\xi+4\nu/m} = \frac{\sigma h_K^2 4\nu/m}{\sigma h_K^2+4\nu/m} \le \frac{\sigma h_K^2 4\nu/m}{\sigma h_K^2} = \frac{4\nu}{m};$$

when $\xi = \frac{4\nu}{m\sigma h_K^2}$ if $4\nu > m\sigma h_K^2$, we have

$$\sigma h_K^2 \frac{\sigma h_K^2(\xi-1)+4\nu/m}{\sigma h_K^2\xi+4\nu/m} = \frac{\sigma h_K^2(8\nu-m\sigma h_K^2)/m}{8\nu/m} \le \sigma h_K^2 < \frac{4\nu}{m}.$$

According to the norms (2.13) and (2.14) and the interpolation properties (3.7) and (3.5), we have

$$\begin{aligned} I_3 &= \sum_{K\in\mathcal{T}_h} (1-\sigma\tau_K)(\nabla(p-\widetilde{p}),\boldsymbol{v})_{0,K} \le c\Big(\sum_{K\in\mathcal{T}_h}(1-\sigma\tau_K)\sigma^{-1}\|\nabla(p-\widetilde{p})\|_{0,K}^2\Big)^{1/2}|\boldsymbol{v}|_{0,h} \\ &\le c\sqrt{\max_{K\in\mathcal{T}_h}\frac{1-\sigma\tau_K}{\sigma\tau_K}}|p-\widetilde{p}|_{1,h}|\boldsymbol{v}|_{0,h} \le c\max_{K\in\mathcal{T}_h}\sqrt{\frac{8\nu}{m\sigma h_K^2}}|p-J_hp|_{1,h}|\boldsymbol{v}|_{0,h} \\ &= c\max_{K\in\mathcal{T}_h}\sqrt{\frac{8\nu}{m\sigma h_K^2}}\Big(\sum_{K\in\mathcal{T}_h}\tau_K\|\nabla(p-J_hp)\|_{0,K}^2\Big)^{1/2}|\boldsymbol{v}|_{0,h} \le c\sqrt{\nu}\frac{h^{\ell-1}}{\sigma}\max_{K\in\mathcal{T}_h}h_K^{-1}|p|_\ell|\boldsymbol{v}|_{0,h}, \end{aligned}$$

where we have used the following estimates

$$\frac{1-\sigma\tau_K}{\sigma\tau_K} \le \frac{8\nu}{m\sigma h_K^2} \quad \text{and} \quad \tau_K \le \frac{1}{\sigma},$$

which can be shown from the function $\xi(\cdot)$.

According to the norm (2.13) and the interpolation property (3.1), we have

$$\begin{aligned} I_4 &= \sum_{K\in\mathcal{T}_h}(1-\sigma\tau_K(\nabla q,\boldsymbol{u}-\widetilde{\boldsymbol{u}})_{0,K} \le \Big(\sum_{K\in\mathcal{T}_h}(1-\sigma\tau_K)^2\tau_K^{-1}\|\boldsymbol{u}-\widetilde{\boldsymbol{u}}\|_{0,K}^2\Big)^{1/2}|q|_{1,h} \\ &\le c\Big(\sum_{K\in\mathcal{T}_h}(1-\sigma\tau_K)^2\tau_K^{-1}h_K^{2(k+1)}|\boldsymbol{u}|_{k+1,K}^2\Big)^{1/2}|q|_{1,h} \le c\sqrt{\nu}h^k|\boldsymbol{u}|_{k+1}|q|_{1,h}, \end{aligned}$$

where we have used the following estimate

$$(1-\sigma\tau_K)^2\tau_K^{-1}h_K^2 \le \frac{8\nu}{m}$$

which can be shown from the function $\xi(\cdot)$.

According to the norm (2.12), the local inverse estimate $Ch_K^2\|\Delta \boldsymbol{v}\|_{0,K}^2 \le \|\nabla \boldsymbol{v}\|_{0,K}^2$, and the interpolation property (3.1), we have

$$\begin{aligned} I_5 &= -\sum_{K\in\mathcal{T}_h}\tau_K(\sigma(\boldsymbol{u}-\widetilde{\boldsymbol{u}}),-\nu\Delta\boldsymbol{v})_{0,K} \le \sum_{K\in\mathcal{T}_h}\sigma\nu\tau_K C^{-1/2}h_K^{-1}\|\boldsymbol{u}-\widetilde{\boldsymbol{u}}\|_{0,K}\|\nabla\boldsymbol{v}\|_{0,K} \\ &\le c\Big(\sum_{K\in\mathcal{T}_h}\sigma^2\nu\tau_K^2C^{-1}h_K^{-2}\|\boldsymbol{u}-\widetilde{\boldsymbol{u}}\|_{0,K}^2\Big)^{1/2}|\boldsymbol{v}|_{1,\nu} \le c\sqrt{\nu}h^k|\boldsymbol{u}|_{k+1}|\boldsymbol{v}|_{1,\nu}, \end{aligned}$$

where we have used the estimate $\sigma\tau_K \le 1$.

According the norm (2.13) and the interpolation property (3.3), we have

$$\begin{aligned} I_6 &= \sum_{K\in\mathcal{T}_h}\tau_K\sigma\nu(\Delta(\boldsymbol{u}-\widetilde{\boldsymbol{u}}),\boldsymbol{v})_{0,K} \\ &\le c\Big(\sum_{K\in\mathcal{T}_h}\frac{\tau_K^2\nu^2\sigma h_K^{-2}}{1-\sigma\tau_K}h_K^2\|\Delta(\boldsymbol{u}-\widetilde{\boldsymbol{u}})\|_{0,K}^2\Big)^{1/2}|\boldsymbol{v}|_{0,h} \le c\sqrt{\nu}h^k|\boldsymbol{u}|_{k+1}|\boldsymbol{v}|_{0,h}, \end{aligned}$$

where we have used the following estimate

$$\frac{\tau_K^2\nu^2\sigma h_K^{-2}}{1-\sigma\tau_K} \le \frac{m\nu}{4}$$

which can be shown from the function $\xi(\cdot)$.

According to the norm (2.12), the local inverse estimate $Ch_K^2\|\Delta \boldsymbol{v}\|_{0,K}^2 \le \|\nabla \boldsymbol{v}\|_{0,K}^2$, and the interpolation property (3.1), we have

$$\begin{aligned} I_7 &\le \sum_{K\in\mathcal{T}_h}\tau_K\nu^2\|\Delta(\boldsymbol{u}-\widetilde{\boldsymbol{u}})\|_{0,K}\|\Delta\boldsymbol{v}\|_{0,K} \le \sum_{K\in\mathcal{T}_h}\tau_K\nu^2C^{-1/2}h_K^{-1}\|\Delta(\boldsymbol{u}-\widetilde{\boldsymbol{u}})\|_{0,K}\|\nabla\boldsymbol{v}\|_{0,K} \\ &\le c\Big(\sum_{K\in\mathcal{T}_h}\tau_K^2h_K^{-4}\nu^3h_K^2\|\Delta(\boldsymbol{u}-\widetilde{\boldsymbol{u}})\|_{0,K}^2\Big)^{1/2}|\boldsymbol{v}|_{1,\nu} \le c\sqrt{\nu}h^k|\boldsymbol{u}|_{k+1}|\boldsymbol{v}|_{1,\nu}, \end{aligned}$$

where we have used the estimate

$$\tau_K^2h_K^{-4}\nu^3 = \frac{\nu^3}{(\sigma h_K^2\xi+4\nu/m)^2} \le \frac{m^2\nu}{16}.$$

According to the norm (2.14) and the interpolation property (3.1), we have

$$I_8 \le \Big(\sum_{K\in\mathcal{T}_h}\tau_Kh_K^{-2}\nu^2h_K^2\|\Delta(\boldsymbol{u}-\widetilde{\boldsymbol{u}})\|_{0,K}^2\Big)^{1/2}|q|_{1,h} \le c\sqrt{\nu}h^k|\boldsymbol{u}|_{k+1}|q|_{1,h},$$

where we have used the following estimate

$$\tau_Kh_K^{-2}\nu^2 = \frac{\nu^2}{\sigma h_K^2\xi+4\nu/m} \le \frac{m\nu}{4}.$$

According to the local inverse estimate $Ch_K^2\|\Delta \boldsymbol{v}\|_{0,K}^2 \leq \|\nabla \boldsymbol{v}\|_{0,K}^2$, the norms (2.14) and (2.12), and the interpolation properties (3.7) and (3.5), we have

$$\begin{aligned} I_9 &\leq \sum_{K\in\mathcal{T}_h} \tau_K \nu \|\nabla(p-\widetilde{p})\|_{0,K}\|\Delta \boldsymbol{v}\|_{0,K} \leq \sum_{K\in\mathcal{T}_h} \tau_K \nu C^{-1/2} h_K^{-1}\|\nabla(p-\widetilde{p})\|_{0,K}\|\nabla \boldsymbol{v}\|_{0,K} \\ &\leq c\Big(\sum_{K\in\mathcal{T}_h} \tau_K^2 \nu h_K^{-2}\|\nabla(p-\widetilde{p})\|_{0,K}^2\Big)^{1/2}|\boldsymbol{v}|_{1,\nu} \leq c\sqrt{\nu}\max_{K\in\mathcal{T}_h}\frac{1}{\sqrt{\sigma h_K^2\xi+4\nu/m}}|p-\widetilde{p}|_{1,h}|\boldsymbol{v}|_{1,\nu} \\ &\leq c\sqrt{\nu}\max_{K\in\mathcal{T}_h}\frac{1}{\sqrt{\sigma h_K^2\xi+4\nu/m}}|p-J_hp|_{1,h}|\boldsymbol{v}|_{1,\nu} \leq c\max_{K\in\mathcal{T}_h}\frac{\sqrt{\nu}}{\sqrt{\sigma}h_K}|p-J_hp|_{1,h}|\boldsymbol{v}|_{1,\nu} \\ &\leq c\sqrt{\nu}\frac{h^{\ell-1}}{\sigma}\max_{K\in\mathcal{T}_h} h_K^{-1}|p|_\ell|\boldsymbol{v}|_{1,\nu}, \end{aligned}$$

where we have used the estimate $\tau_K \leq \sigma^{-1}$ (see the proof of I_3).

Finally, considering the last term I_{10}, from the definition (3.6) of $\widetilde{p}$, we have

$$I_{10} = -\sum_{K\in\mathcal{T}_h} \tau_K(\nabla(p-\widetilde{p}),\nabla q)_{0,K} = 0.$$

Summarizing all the above estimates and the obvious inequality $\|(\boldsymbol{v},q)\|_h \leq |||(\boldsymbol{v},q)|||_h$, we have

$$\begin{aligned} \boldsymbol{B}((\boldsymbol{w},z),(\boldsymbol{v},q)) &\leq c\sqrt{\nu}\Big(h^k|\boldsymbol{u}|_{k+1}+\frac{h^{\ell-1}}{\sigma}\max_{K\in\mathcal{T}_h} h_K^{-1}|p|_\ell\Big)\|(\boldsymbol{v},q)\|_h \\ &\leq c\sqrt{\nu}\Big(h^k|\boldsymbol{u}|_{k+1}+\frac{h^{\ell-1}}{\sigma}\max_{K\in\mathcal{T}_h} h_K^{-1}|p|_\ell\Big)|||(\boldsymbol{v},q)|||_h, \end{aligned}$$

and from (3.9) we obtain

$$|||(\boldsymbol{w},z)|||_h \leq c\sqrt{\nu}\Big(h^k|\boldsymbol{u}|_{k+1}+\frac{h^{\ell-1}}{\sigma}\max_{K\in\mathcal{T}_h} h_K^{-1}|p|_\ell\Big). \tag{3.10}$$

The desired results thus follow. This completes the proof. □

The two significant features for the *standard* H^1 semi-norm errors of the velocity in Lemma 3.1 are that the viscosity ν, which is usually small, completely disappears and the reaction constant σ, which is usually large, acts only in the denominator position.

Remark 3.2. *If the pressure p is more regular, say $p \in H^{\ell+1}(\Omega)$, then all the estimates in Lemma 3.1 can be obtained as follows:*

$$\begin{aligned} \|\nabla(\boldsymbol{u}_h-\widetilde{\boldsymbol{u}})\|_0 &\leq c\Big(h^k|\boldsymbol{u}|_{k+1}+\frac{h^\ell}{\sigma}\max_{K\in\mathcal{T}_h} h_K^{-1}|p|_{\ell+1}\Big), \\ |\boldsymbol{u}_h-\widetilde{\boldsymbol{u}}|_{0,h} &\leq c\sqrt{\nu}\Big(h^k|\boldsymbol{u}|_{k+1}+\frac{h^\ell}{\sigma}\max_{K\in\mathcal{T}_h} h_K^{-1}|p|_{\ell+1}\Big), \\ |p_h-\widetilde{p}|_{1,h} &\leq c\sqrt{\nu}\Big(h^k|\mathbf{u}|_{k+1}+\frac{h^\ell}{\sigma}\max_{K\in\mathcal{T}_h} h_K^{-1}|p|_{\ell+1}\Big), \\ \|p_h-\widetilde{p}\|_0 &\leq c\sqrt{(\sigma+\nu)\nu}\Big(h^k|\boldsymbol{u}|_{k+1}+\frac{h^\ell}{\sigma}\max_{K\in\mathcal{T}_h} h_K^{-1}|p|_{\ell+1}\Big). \end{aligned}$$

The main purpose of Lemma 3.1 is for the establishment of the effects on the convergence of the finite element solutions from the physical parameters σ and ν, so these error estimates are not established in terms of the optimum in h with respect to the order of approximations. However, as reviewed in the introduction section, from the error estimates which is obtained by [3], the optimum in h indeed holds in the convergence if one does not care the values of σ and ν. On the other hand, we can obtain more general error estimates from the argument in proving Lemma 3.1. For that goal, we choose $\widetilde{p} := J_h p$ which satisfies (3.4) and (3.5), instead of the finite element projection given in (3.6), because we need the L^2 norm error estimates for $p - \widetilde{p}$. As mentioned in Remark 3.1, such error estimates are not available for (3.6). While other terms are estimated unchanged as in proving Lemma 3.1, we therefore only re-estimate the following four terms:

$$-(p-\widetilde{p}, \nabla \cdot \boldsymbol{v}), \quad -\sum_{K\in\mathcal{T}_h} \tau_K(\nabla(p-\widetilde{p}), \sigma\boldsymbol{v})_{0,K},$$

$$-\sum_{K\in\mathcal{T}_h} \tau_K(\nabla(p-\widetilde{p}), -\nu\Delta\boldsymbol{v})_{0,K}, \quad -\sum_{K\in\mathcal{T}_h} \tau_K(\nabla(p-\widetilde{p}), \nabla q)_{0,K}.$$

From (3.4) and (3.5), we have the following estimates:

$$-(p-\widetilde{p}, \nabla\cdot\boldsymbol{v}) \le \|p-\widetilde{p}\|_0 \|\nabla \boldsymbol{v}\|_0 \le c\frac{h^\ell}{\sqrt{\nu}} |p|_\ell |\boldsymbol{v}|_{1,\nu}$$

and

$$\begin{aligned} -\sum_{K\in\mathcal{T}_h} \tau_K(\nabla(p-\widetilde{p}), \sigma\boldsymbol{v})_{0,K} &\le c\Big(\sum_{K\in\mathcal{T}_h} \frac{\sigma\tau_K^2}{1-\sigma\tau_K}\|\nabla(p-\widetilde{p})\|_{0,K}^2\Big)^{1/2} |\boldsymbol{v}|_{0,h} \\ &\le c\frac{h^\ell}{\sqrt{4\nu/m}}|p|_\ell |\boldsymbol{v}|_{0,h}, \end{aligned}$$

where we have used the interpolation error estimate (3.5) for $s = \ell$ and $\sigma\tau_K^2/(1-\sigma\tau_K) \le 1/(4\nu/m)$ which can be shown by the two choices $\xi = 1$ and $\xi = 4\nu/(m\sigma h_K^2)$. In the following two estimates, we have used the interpolation error estimate (3.5) for $s = \ell$, the local inverse $Ch_K^2\|\Delta\boldsymbol{v}\|_{0,K}^2 \le \|\nabla\boldsymbol{v}\|_{0,K}^2$ and the fact that $\tau_K \le h_K^2/(4\nu/m)$:

$$\begin{aligned} -\sum_{K\in\mathcal{T}_h} \tau_K(\nabla(p-\widetilde{p}), -\nu\Delta\boldsymbol{v})_{0,K} &\le \sum_{K\in\mathcal{T}_h} \nu\tau_K C^{-1/2} h_K^{-1} \|\nabla(p-\widetilde{p})\|_{0,K}\|\nabla\boldsymbol{v}\|_{0,K} \\ &\le c\frac{h^\ell}{\sqrt{4\nu/m}}|p|_\ell|\boldsymbol{v}|_{1,\nu} \end{aligned}$$

and

$$-\sum_{K\in\mathcal{T}_h} \tau_K(\nabla(p-\widetilde{p}), \nabla q)_{0,K} \le c\frac{h^\ell}{\sqrt{4\nu/m}}|p|_\ell |q|_{1,h}.$$

Hence, with the same $(\boldsymbol{w}, z)$ as in Lemma 3.1, we have

$$|||(\boldsymbol{w}, z)|||_h \le c\Big(\sqrt{\nu}h^k|\boldsymbol{u}|_{k+1} + \frac{h^\ell}{\sqrt{4\nu/m}}|p|_\ell\Big). \tag{3.11}$$

Thus, we have proven the following lemma which states the optimum in h relative to the order of approximations. Also, the dependence on σ and ν are explicitly revealed.

Lemma 3.2. *Under the same assumptions as in Lemma 3.1, only with the replacement $\widetilde{p}$ by the nodal interpolation $J_h p$ which satisfies (3.4) and (3.5), we have*

$$\begin{aligned}
\|\nabla(\boldsymbol{u}_h - \widetilde{\boldsymbol{u}})\|_0 &\leq c\Big(h^k|\boldsymbol{u}|_{k+1} + \frac{h^\ell}{4\nu/m}|p|_\ell\Big),\\
|\boldsymbol{u}_h - \widetilde{\boldsymbol{u}}|_{0,h} &\leq c\Big(\sqrt{\nu}h^k|\boldsymbol{u}|_{k+1} + \frac{h^\ell}{\sqrt{4\nu/m}}|p|_\ell\Big),\\
|p_h - \widetilde{p}|_{1,h} &\leq c\Big(\sqrt{\nu}h^k|\boldsymbol{u}|_{k+1} + \frac{h^\ell}{\sqrt{4\nu/m}}|p|_\ell\Big),\\
\|p_h - \widetilde{p}\|_0 &\leq c\sqrt{\sigma+\nu}\Big(\sqrt{\nu}h^k|\boldsymbol{u}|_{k+1} + \frac{h^\ell}{\sqrt{4\nu/m}}|p|_\ell\Big).
\end{aligned}$$

If, additionally, $p \in H^{\ell+1}(\Omega)$, we have

$$\begin{aligned}
\|\nabla(\boldsymbol{u}_h - \widetilde{\boldsymbol{u}})\|_0 &\leq c\Big(h^k|\boldsymbol{u}|_{k+1} + \frac{h^{\ell+1}}{4\nu/m}|p|_{\ell+1}\Big),\\
|\boldsymbol{u}_h - \widetilde{\boldsymbol{u}}|_{0,h} &\leq c\Big(\sqrt{\nu}h^k|\boldsymbol{u}|_{k+1} + \frac{h^{\ell+1}}{\sqrt{4\nu/m}}|p|_{\ell+1}\Big),\\
|p_h - \widetilde{p}|_{1,h} &\leq c\Big(\sqrt{\nu}h^k|\boldsymbol{u}|_{k+1} + \frac{h^{\ell+1}}{\sqrt{4\nu/m}}|p|_{\ell+1}\Big),\\
\|p_h - \widetilde{p}\|_0 &\leq c\sqrt{\sigma+\nu}\Big(\sqrt{\nu}h^k|\boldsymbol{u}|_{k+1} + \frac{h^{\ell+1}}{\sqrt{4\nu/m}}|p|_{\ell+1}\Big).
\end{aligned}$$

Now we state the main result of the H^1 semi-norm error estimates of the velocity.

Theorem 3.1. *Let $(\boldsymbol{u}_h, p_h) \in \boldsymbol{V}_h \times Q_h$ denote the finite element solution pair to problem (2.8). Assume that the exact solution pair $(\boldsymbol{u}, p) \in (H^{k+1}(\Omega) \cap H_0^1(\Omega))^d \times (H^\ell(\Omega) \cap L_0^2(\Omega))$ for $k, \ell \geq 1$. Assuming quasi-uniform meshes with $h_K \geq ch$, we have*

$$\|\nabla(\boldsymbol{u} - \boldsymbol{u}_h)\|_0 \leq c\Big(h^k|\boldsymbol{u}|_{k+1} + \frac{h^\ell}{\max\{\sigma h^2, 4\nu/m\}}|p|_\ell\Big).$$

If, additionally, $p \in H^{l+1}(\Omega)$, we have

$$\|\nabla(\boldsymbol{u} - \boldsymbol{u}_h)\|_0 \leq c\Big(h^k|\boldsymbol{u}|_{k+1} + \frac{h^{\ell+1}}{\max\{\sigma h^2, 4\nu/m\}}|p|_{\ell+1}\Big).$$

Proof. Applying the triangle inequality, we obtain the error estimates from Lemma 3.1, the interpolation property (3.2) of $\boldsymbol{I}_h\boldsymbol{u}$, the assumption $h_K \geq ch$, Lemma 3.2, and Remark 3.2. □

The assumption of quasi-uniform meshes with $h_K \geq ch$ is due to the presence of $\max_{K\in\mathcal{T}_h} h_K^{-1}$ in Lemma 3.1, while such an assumption is not needed in Lemma 3.2. So far, we have obtained the error bound in H^1 semi-norm for the velocity, whatever the values of σ, ν and h are.

From Lemma 3.1 and the assumption of quasi-uniform meshes, we can obtain error estimates of the velocity in L^2-norm and of the pressure. In fact, we first remark that, due to quasi-uniform meshes with $h_K \geq ch$, there hold

$$c_9 \leq \max_{K\in\mathcal{T}_h} \tau_K \Big/ \min_{K\in\mathcal{T}_h} \tau_K \leq c_{10} \tag{3.12}$$

and

$$c_{11} \le \max_{K\in\mathcal{T}_h}(1-\sigma\tau_K)\Big/\min_{K\in\mathcal{T}_h}(1-\sigma\tau_K) \le c_{12}. \tag{3.13}$$

From the estimates in the norm $|\cdot|_{0,h}$ of $\boldsymbol{u}_h - \widetilde{\boldsymbol{u}}$ in Lemma 3.1 and Lemma 3.2 and (3.13), we obtain

$$\|\boldsymbol{u}_h - \widetilde{\boldsymbol{u}}\|_0 \le c\sqrt{\frac{h^2}{4\nu/m} + \frac{1}{\sigma}}\Big(\sqrt{\nu}h^k|\boldsymbol{u}|_{k+1} + \frac{h^\ell}{\max\{\sigma h^2/\sqrt{4\nu/m}, \sqrt{4\nu/m}\}}|p|_\ell\Big),$$

and by considering the two cases $4\nu \le m\sigma h^2$ and $4\nu > m\sigma h^2$, we further obtain

$$\|\boldsymbol{u}_h - \widetilde{\boldsymbol{u}}\|_0 \le c\Big(\max\Big\{1, \sqrt{\frac{4\nu}{m\sigma h^2}}\Big\}h^{k+1}|\boldsymbol{u}|_{k+1} + \frac{h^\ell}{\sigma h}|p|_\ell\Big).$$

By applying the triangle inequality and the interpolation property (3.1), we then conclude the following results of the L^2 norm error estimates of the velocity.

Corollary 3.1. *Under the same assumptions as in Theorem 3.1, we have*

$$\begin{aligned}
\|\boldsymbol{u} - \boldsymbol{u}_h\|_0 &\le c\Big(\max\Big\{1, \sqrt{\frac{4\nu}{m\sigma h^2}}\Big\}h^{k+1}|\boldsymbol{u}|_{k+1} + \frac{h^\ell}{\sigma h}|p|_\ell\Big),\\
\|\boldsymbol{u} - \boldsymbol{u}_h\|_0 &\le c\Big(\max\Big\{1, \sqrt{\frac{4\nu}{m\sigma h^2}}\Big\}h^{k+1}|\boldsymbol{u}|_{k+1} + \frac{h^{\ell+1}}{\sigma h}|p|_{\ell+1}\Big).
\end{aligned}$$

We see that the reaction constant σ acts only in the denominator position while the viscosity ν in the numerator position. When compared with Theorem 3.1, we find that $\|\boldsymbol{u} - \boldsymbol{u}_h\|_0$ behaves one order higher than the H^1 semi-norm errors. We should point out that we have not assumed a convex Ω for which the Aubin-Nitsche duality argument can be applied.

Regarding the pressure, from Lemma 3.1, Lemma 3.2, (3.7), (3.5) and (3.12), we can obtain

$$\|\nabla(p_h - p)\|_0 \le c\sqrt{\frac{4\nu}{m} + \sigma h^2}\Big(\sqrt{\nu}h^{k-1}|\boldsymbol{u}|_{k+1} + \frac{h^{\ell-1}}{\max\{\sigma h^2/\sqrt{4\nu/m}, \sqrt{4\nu/m}\}}|p|_\ell\Big),$$

and considering the two cases $4\nu \le m\sigma h^2$ and $4\nu > m\sigma h^2$, we have

$$\|\nabla(p_h - p)\|_0 \le c\Big(\max\Big\{1, \sqrt{\frac{4\nu}{m\sigma h^2}}\Big\}h^{\ell-1}|p|_\ell + \max\Big\{\sqrt{\sigma h^2}, \sqrt{\frac{4\nu}{m}}\Big\}\sqrt{\nu}h^{k-1}|\boldsymbol{u}|_{k+1}\Big). \tag{3.14}$$

In the second term of (3.14), σ lives in the numerator position. In order to establish better error estimates, with σ acting in the denominator position only, we shall resort to a different way.

We first note that the factor τ_K in $|q|_{1,h}$-norm can be dealt with as a whole, due to (3.12). As a result, for the finite element projection $\widetilde{p}$ given by (3.6), we have from (3.7)

$$\|\nabla(p - \widetilde{p})\|_0 \le c\|\nabla(p - J_h p)\|_0. \tag{3.15}$$

In what follows, we shall give the error estimates for the pressure. For that goal, we need a different interpolation for $\boldsymbol{u}$, instead of the nodal-interpolation $\widetilde{\boldsymbol{u}} = \boldsymbol{I}_h\boldsymbol{u}$. We define the interpolation $\widetilde{\boldsymbol{u}} \in \boldsymbol{V}_h$ as the finite element projection of $\boldsymbol{u}$ in the following:

$$\begin{aligned}
&\sigma(\widetilde{\boldsymbol{u}}, \boldsymbol{v}) + \nu(\nabla\widetilde{\boldsymbol{u}}, \nabla\boldsymbol{v}) - \sum_{K\in\mathcal{T}_h}\tau_K(\sigma\widetilde{\boldsymbol{u}} - \nu\Delta\widetilde{\boldsymbol{u}}, \sigma\boldsymbol{v} - \nu\Delta\boldsymbol{v})_{0,K}\\
&\quad= \sigma(\boldsymbol{u}, \boldsymbol{v}) + \nu(\nabla\boldsymbol{u}, \nabla\boldsymbol{v}) - \sum_{K\in\mathcal{T}_h}\tau_K(\sigma\boldsymbol{u} - \nu\Delta\boldsymbol{u}, \sigma\boldsymbol{v} - \nu\Delta\boldsymbol{v})_{0,K}.
\end{aligned} \tag{3.16}$$

Problem (3.16) allows a unique solution $\widetilde{\boldsymbol{u}} \in \boldsymbol{V}_h$. Following a similar argument for proving Lemma 3.1, we can obtain the following error estimates:

$$\|\nabla(\boldsymbol{u}-\widetilde{\boldsymbol{u}})\|_0 \leq ch^k|\boldsymbol{u}|_{k+1}, \tag{3.17}$$

$$|\boldsymbol{u}-\widetilde{\boldsymbol{u}}|_{0,h} \leq c\sqrt{\nu}h^k|\boldsymbol{u}|_{k+1}. \tag{3.18}$$

Under the assumption of quasi-uniform meshes, we have

$$\Big(\sum_{K\in\mathcal{T}_h}\|\Delta(\boldsymbol{u}-\widetilde{\boldsymbol{u}})\|_{0,K}^2\Big)^{1/2} \leq ch^{k-1}|\boldsymbol{u}|_{k+1}.$$

Using this $\widetilde{\boldsymbol{u}}$ and following the argument in proving Lemma 3.1, with $(\boldsymbol{w},z)=(\boldsymbol{u}_h-\widetilde{\boldsymbol{u}},p_h-\widetilde{p})$, we have

$$\begin{aligned}
&\boldsymbol{B}((\boldsymbol{w},z),(\boldsymbol{v},q)) = \boldsymbol{B}((\boldsymbol{u}-\widetilde{\boldsymbol{u}},p-\widetilde{p}),(\boldsymbol{v},q))\\
&= -(p-\widetilde{p},\nabla\cdot\boldsymbol{v}) - (q,\nabla\cdot(\boldsymbol{u}-\widetilde{\boldsymbol{u}}))\\
&\quad -\sum_{K\in\mathcal{T}_h}\tau_K(\sigma(\boldsymbol{u}-\widetilde{\boldsymbol{u}})-\nu\Delta(\boldsymbol{u}-\widetilde{\boldsymbol{u}}),\nabla q)_{0,K} - \sum_{K\in\mathcal{T}_h}\tau_K(\nabla(p-\widetilde{p}),\sigma\boldsymbol{v}-\nu\Delta\boldsymbol{v})_{0,K}\\
&= \sum_{K\in\mathcal{T}_h}(1-\sigma\tau_K)(\boldsymbol{v},\nabla(p-\widetilde{p}))_{0,K} + \sum_{K\in\mathcal{T}_h}(1-\sigma\tau_K)(\boldsymbol{u}-\widetilde{\boldsymbol{u}},\nabla q)_{0,K}\\
&\quad +\sum_{K\in\mathcal{T}_h}\nu\tau_K(\Delta(\boldsymbol{u}-\widetilde{\boldsymbol{u}}),\nabla q)_{0,K} + \sum_{K\in\mathcal{T}_h}\nu\tau_K(\Delta\boldsymbol{v},\nabla(p-\widetilde{p}))_{0,K}\\
&\leq c|||(\boldsymbol{v},q)|||_h\Bigg(\sqrt{\max_{K\in\mathcal{T}_h}\sigma^{-1}(1-\sigma\tau_K)}\|\nabla(p-\widetilde{p})\|_0 + \sqrt{\max_{K\in\mathcal{T}_h}\sigma^{-1}\tau_K^{-1}(1-\sigma\tau_K)}|\boldsymbol{u}-\widetilde{\boldsymbol{u}}|_{0,h}\\
&\qquad +\nu\sqrt{\max_{K\in\mathcal{T}_h}\tau_K}\Big(\sum_{K\in\mathcal{T}_h}\|\Delta(\boldsymbol{u}-\widetilde{\boldsymbol{u}})\|_{0,K}^2\Big)^{1/2} + \sqrt{\max_{K\in\mathcal{T}_h}\nu h_K^{-2}\tau_K^2}\|\nabla(p-\widetilde{p})\|_0\Bigg).
\end{aligned} \tag{3.19}$$

From the definition of $|||(\cdot,\cdot)|||_h$, under the assumption of quasi-uniform meshes (i.e., $h_K \geq ch$), we obtain from the stability (3.9)

$$\begin{aligned}
&c\sqrt{\min_{K\in\mathcal{T}_h}\tau_K}\|\nabla(p_h-\widetilde{p})\|_0\\
&\leq \sqrt{\max_{K\in\mathcal{T}_h}\sigma^{-1}(1-\sigma\tau_K)}\|\nabla(p-\widetilde{p})\|_0 + \sqrt{\max_{K\in\mathcal{T}_h}\sigma^{-1}\tau_K^{-1}(1-\sigma\tau_K)}|\boldsymbol{u}-\widetilde{\boldsymbol{u}}|_{0,h}\\
&\quad +\nu\sqrt{\max_{K\in\mathcal{T}_h}\tau_K}\Big(\sum_{K\in\mathcal{T}_h}\|\Delta(\boldsymbol{u}-\widetilde{\boldsymbol{u}})\|_{0,K}^2\Big)^{1/2} + \sqrt{\max_{K\in\mathcal{T}_h}\nu h_K^{-2}\tau_K^2}\|\nabla(p-\widetilde{p})\|_0,
\end{aligned}$$

and, from the interpolation error estimates: (3.15), (3.5), (3.3), (3.17) and (3.18), we further obtain

$$\begin{aligned}
&c\|\nabla(p_h-\widetilde{p})\|_0 \leq \max_{K\in\mathcal{T}_h}\sqrt{\frac{\sigma h_K^2(\xi-1)+4\nu/m}{\sigma h_K^2}}\|\nabla(p-J_hp)\|_0\\
&\quad +\max_{K\in\mathcal{T}_h}\sqrt{\frac{\sigma h_K^2(\xi-1)+4\nu/m}{\sigma h_K^2}}\sqrt{\frac{\sigma h_K^2\xi+4\nu/m}{h_K^2}}|\boldsymbol{u}-\widetilde{\boldsymbol{u}}|_{0,h}\\
&\quad +\nu\Big(\sum_{K\in\mathcal{T}_h}\|\Delta(\boldsymbol{u}-\widetilde{\boldsymbol{u}})\|_{0,K}^2\Big)^{1/2} + \max_{K\in\mathcal{T}_h}\sqrt{\frac{\nu}{\sigma h_K^2\xi+4\nu/m}}\|\nabla(p-J_hp)\|_0\\
&\leq \sqrt{\frac{4\nu}{m\sigma h^2}}h^{\ell-1}|p|_\ell + \max\Big\{(1,\sqrt{\frac{4\nu}{m\sigma h^2}}\Big\}\nu h^{k-1}|\boldsymbol{u}|_{k+1} + \nu h^{k-1}|\boldsymbol{u}|_{k+1} + h^{\ell-1}|p|_\ell,
\end{aligned} \tag{3.20}$$

that is

$$\|\nabla(p_h-\widetilde{p})\|_0 \le c\max\Big\{1,\sqrt{\frac{4\nu}{m\sigma h^2}}\Big\}\Big(h^{\ell-1}|p|_\ell+\nu h^{k-1}|\boldsymbol{u}|_{k+1}\Big).$$

Thus, we can conclude the following corollary.

Corollary 3.2. *Under the same assumptions as in Lemma 3.1 and the quasi-uniform assumption of $h_K \ge ch$, we have*

$$\|\nabla(p_h-p)\|_0 \le c\max\Big\{1,\sqrt{\frac{4\nu}{m\sigma h^2}}\Big\}\Big(h^{\ell-1}|p|_\ell+\nu h^{k-1}|\boldsymbol{u}|_{k+1}\Big).$$

If $p \in H^{\ell+1}(\Omega)$, we can similarly obtain

$$\|\nabla(p_h-p)\|_0 \le c\max\Big\{1,\sqrt{\frac{4\nu}{m\sigma h^2}}\Big\}\Big(h^{\ell}|p|_{\ell+1}+\nu h^{k-1}|\boldsymbol{u}|_{k+1}\Big).$$

Again, for pressure, the viscosity constant acts only in the numerator position while the reaction constant σ in the denominator position.

Now, taking $\widetilde{\boldsymbol{u}} = \boldsymbol{I}_h\boldsymbol{u}$ satisfying (3.1), (3.2) and (3.3) and $\widetilde{p} = J_h p$ satisfying (3.4) and (3.5). From Lemma 3.2, we obtain

$$\|\nabla(p_h-p)\|_0 \le c\max\Big\{1,\sqrt{\frac{m\sigma h^2}{4\nu}}\Big\}\Big(h^{\ell-1}|p|_\ell+\nu h^{k-1}|\boldsymbol{u}|_{k+1}\Big), \tag{3.21}$$

$$\|\nabla(p_h-p)\|_0 \le c\max\Big\{1,\sqrt{\frac{m\sigma h^2}{4\nu}}\Big\}\Big(h^{\ell}|p|_{\ell+1}+\nu h^{k-1}|\boldsymbol{u}|_{k+1}\Big). \tag{3.22}$$

Hence, combining Corollary 3.2 and (3.21) and (3.22), we conclude the following main result of the H^1 semi-norm error estimates of the pressure.

Theorem 3.2. *Under the same assumptions as in Corollary 3.2, there hold*

$$\begin{aligned}\|\nabla(p_h-p)\|_0 &\le c\Big(h^{\ell-1}|p|_\ell+\nu h^{k-1}|\boldsymbol{u}|_{k+1}\Big),\\ \|\nabla(p_h-p)\|_0 &\le c\Big(h^{\ell}|p|_{\ell+1}+\nu h^{k-1}|\boldsymbol{u}|_{k+1}\Big).\end{aligned}$$

The significant feature of the H^1 semi-norm error estimates in Theorem 3.2 for the pressure is that they are independent of σ. Although the regularity of the exact solution pair $(\boldsymbol{u}, p)$ usually depend on σ and ν, Theorem 3.2 indicates that the numerical behavior of the H^1 semi-norm of p_h will not be affected from σ and ν (if $\nu \le c$). This feature has been numerically confirmed in [3].

Remark 3.3. *All the error estimates which have obtained so far are essentially uniform, up to the regularity-norms of the exact solution pair $(\boldsymbol{u}, p)$, since the viscosity constant ν and the reaction constant σ act in the numerator position and the denominator position, respectively.*

4. L^2 Error Estimates of the Velocity in Convex Ω

As we have seen, the L^2 norm error estimates of the velocity can behave with one order higher than the H^1 semi-norm error estimates, regardless of the values of σ, ν and h and without the application of the classical Aubin-Nitsche duality argument. On the other hand, the L^2 norm errors of the velocity obtained in the previous section are not applicable for the case of $\sigma = 0$. So, the purpose of this section is twofold: when Ω is convex for which the Aubin-Nitsche duality argument can apply, the L^2 norm error estimates of the velocity are established with one order higher than the H^1 semi-norm error estimates in Theorem 3.1 and are valid in the case $\sigma = 0$. We remark that if $\sigma = 0$ then the element-wise stabilization parameter τ_K defined in (2.4) should be simplified to $\tau_K = h_K^2/(8\nu/m_k)$.

As usual, we consider the auxiliary problem: *Find* $(\boldsymbol{u}^*, p^*) \in (H_0^1(\Omega))^d \times L_0^2(\Omega)$ *such that*

$$\left\{\begin{array}{rcl} -\nu\Delta \boldsymbol{u}^* + \nabla p^* + \sigma \boldsymbol{u}^* &=& \boldsymbol{u} - \boldsymbol{u}_h \quad \text{in } \Omega, \\ \nabla \cdot \boldsymbol{u}^* &=& 0 \quad \text{in } \Omega, \\ \boldsymbol{u}^* &=& \boldsymbol{0} \quad \text{on } \Gamma, \end{array}\right. \tag{4.1}$$

where $\boldsymbol{u}$ is the velocity of the solution pair $(\boldsymbol{u}, p)$ to problem (1.1) and $\boldsymbol{u}_h \in \boldsymbol{V}_h$ is the velocity of the finite element solution pair $(\boldsymbol{u}_h, p_h)$ of problem (2.8). We shall require that there holds the following regularity:

$$\nu\|\boldsymbol{u}^*\|_2 + \|p^*\|_1 \le c\|\boldsymbol{u} - \boldsymbol{u}_h\|_0. \tag{4.2}$$

When Ω is a two dimensional convex polygon, the above can be shown relatively easily by means of the stream function approach. In three dimensions, (4.2) would also hold.

Put $e^u = \boldsymbol{u} - \boldsymbol{u}_h$ and $e^p = p - p_h$, where p is the pressure of the solution pair $(\boldsymbol{u}, p)$ of problem (1.1) and $p_h \in Q_h$ the pressure of the finite element solution pair $(\boldsymbol{u}_h, p_h)$ of problem (2.8). Let $(\boldsymbol{u}_h^*, p_h^*) = (\boldsymbol{I}_h \boldsymbol{u}, J_h p) \in \boldsymbol{V}_h \times Q_h$ which are the nodal interpolations satisfying (3.1)-(3.5). We have

$$\begin{aligned} \|e^u\|_0^2 \;=\;& \nu(\nabla(\boldsymbol{u}^* - \boldsymbol{u}_h^*), \nabla e^u) + \sigma(\boldsymbol{u}^* - \boldsymbol{u}_h^*, e^u) + (\nabla(p^* - p_h^*), e^u) - (e^p, \nabla\cdot(\boldsymbol{u}^* - \boldsymbol{u}_h^*)) \\ & + \nu(\nabla \boldsymbol{u}_h^*, \nabla e^u) + \sigma(\boldsymbol{u}_h^*, e^u) + (\nabla p_h^*, e^u) - (e^p, \nabla\cdot \boldsymbol{u}_h^*). \end{aligned}$$

From the orthogonality property (3.8), we have

$$\begin{aligned} & \nu(\nabla \boldsymbol{u}_h^*, \nabla e^u) + \sigma(\boldsymbol{u}_h^*, e^u) + (\nabla p_h^*, e^u) - (e^p, \nabla\cdot \boldsymbol{u}_h^*) \\ &= \sum_{K\in\mathcal{T}_h} \tau_K\Big(\sigma e^u - \nu\Delta e^u + \nabla e^p, \sigma \boldsymbol{u}_h^* - \nu\Delta \boldsymbol{u}_h^* + \nabla p_h^*\Big)_{0,K} \\ &= -\sum_{K\in\mathcal{T}_h} \tau_K\Big(\sigma e^u - \nu\Delta e^u + \nabla e^p, \sigma(\boldsymbol{u}^* - \boldsymbol{u}_h^*) - \nu\Delta(\boldsymbol{u}^* - \boldsymbol{u}_h^*) + \nabla(p^* - p_h^*)\Big)_{0,K} \\ & \quad + \sum_{K\in\mathcal{T}_h} \tau_K\Big(\sigma e^u - \nu\Delta e^u + \nabla e^p, \sigma \boldsymbol{u}^* - \nu\Delta \boldsymbol{u}^* + \nabla p^*\Big)_{0,K}, \end{aligned}$$

but, from the first equation of (4.1), we have $\sigma \boldsymbol{u}^* - \nu\Delta \boldsymbol{u}^* + \nabla p^* = e^u$, and we have

$$\begin{aligned} \|e^u\|_0^2 \;=\;& \nu(\nabla(\boldsymbol{u}^* - \boldsymbol{u}_h^*), \nabla e^u) + \sigma(\boldsymbol{u}^* - \boldsymbol{u}_h^*, e^u) + (\nabla(p^* - p_h^*), e^u) - (e^p, \nabla\cdot(\boldsymbol{u}^* - \boldsymbol{u}_h^*)) \\ & - \sum_{K\in\mathcal{T}_h} \tau_K\Big(\sigma e^u - \nu\Delta e^u + \nabla e^p, \sigma(\boldsymbol{u}^* - \boldsymbol{u}_h^*) - \nu\Delta(\boldsymbol{u}^* - \boldsymbol{u}_h^*) + \nabla(p^* - p_h^*)\Big)_{0,K} \\ & + \sum_{K\in\mathcal{T}_h} \tau_K\Big(\sigma e^u - \nu\Delta e^u + \nabla e^p, e^u\Big)_{0,K}. \end{aligned}$$

We first estimate the last term in the above. We expand it as

$$\sum_{K\in\mathcal{T}_h} \tau_K(\sigma e^u - \nu\Delta e^u + \nabla e^p, e^u)_{0,K} = \sum_{K\in\mathcal{T}_h} \sigma\tau_K\|e^u\|_{0,K}^2 - \sum_{K\in\mathcal{T}_h} \nu\tau_K(\Delta e^u, e^u)_{0,K} + \sum_{K\in\mathcal{T}_h} \tau_K(\nabla e^p, e^u)_{0,K}.$$

The three terms in the above are estimated as follows. From the finite element interpolation properties (3.1), (3.2), (3.5), (3.3) and Lemma 3.2, since $\sigma(1-\sigma\tau_K) \leq ch_K^{-1}\sqrt{\nu}$ which can be shown by the two choices $\xi = 1$ for $4\nu \leq m\sigma h_K^2$ and $\xi = 4\nu/(m\sigma h_K^2)$ for $4\nu > m\sigma h_K^2$, we have

$$|\boldsymbol{u} - \boldsymbol{I}_h\boldsymbol{u}|_{0,h} \leq c\sqrt{\nu}h^k|\boldsymbol{u}|_{k+1},$$

and we have

$$|e^u|_{0,h} \leq |\boldsymbol{u} - \boldsymbol{I}_h\boldsymbol{u}|_{0,h} + |\boldsymbol{I}_h\boldsymbol{u} - \boldsymbol{u}_h|_{0,h} \leq c\Big(\sqrt{\nu}h^k|\boldsymbol{u}|_{k+1} + \frac{h^\ell}{\sqrt{4\nu/m}}|p|_\ell\Big),$$

and, since $\sigma\tau_K^2/(1-\sigma\tau_K) \leq ch_K/\sqrt{4\nu/m}$, we have

$$\begin{aligned}\sum_{K\in\mathcal{T}_h}\sigma\tau_K\|e^u\|_{0,K}^2 &\leq \Big(\sum_{K\in\mathcal{T}_h}\sigma^2\tau_K^2\|e^u\|_{0,K}^2\Big)^{1/2}\|e^u\|_0 \leq \sqrt{\max_{K\in\mathcal{T}_h}\frac{\sigma\tau_K^2}{1-\sigma\tau_K}}|e^u|_{0,h}\|e^u\|_0 \\ &\leq c\Big(h^{k+1}|\boldsymbol{u}|_{k+1} + \frac{h^{\ell+1}}{4\nu/m}|p|_\ell\Big)\|e^u\|_0.\end{aligned}$$

Since $\nu\tau_K \leq ch_K^2$, we have no difficulties in obtaining the estimates of the other terms,

$$\begin{aligned}-\sum_{K\in\mathcal{T}_h}\nu\tau_K(\Delta e^u, e^u)_{0,K} &\leq \Big(\sum_{K\in\mathcal{T}_h}\nu^2\tau_K^2\|\Delta(\boldsymbol{u} - \boldsymbol{I}_h\boldsymbol{u})\|_{0,K}^2\Big)^{1/2}\|e^u\|_0 \\ &\quad +\Big(\sum_{K\in\mathcal{T}_h}\nu^2\tau_K^2h_K^{-2}\|\nabla(\boldsymbol{I}_h\boldsymbol{u} - \boldsymbol{u}_h)\|_{0,K}^2\Big)^{1/2}\|e^u\|_0 \\ &\leq c\Big(h^{k+1}|\boldsymbol{u}|_{k+1} + \frac{h^{\ell+1}}{4\nu/m}|p|_\ell\Big)||e^u||_0,\end{aligned}$$

and

$$\sum_{K\in\mathcal{T}_h}\tau_K(\nabla e^p, e^u)_{0,K} \leq \Big(\sum_{K\in\mathcal{T}_h}\tau_K^2\|\nabla e^p\|_{0,K}^2\Big)^{1/2}\|e^u\|_0 \leq c\Big(h^{k+1}|\boldsymbol{u}|_{k+1} + \frac{h^{\ell+1}}{4\nu/m}|p|_\ell\Big)\|e^u\|_0.$$

Hence,

$$\|e^u\|_0^2 \leq |E| + c\Big(h^{k+1}|\boldsymbol{u}|_{k+1} + \frac{h^{\ell+1}}{4\nu/m}|p|_\ell\Big)\|e^u\|_0,$$

where E is defined as

$$\begin{aligned}E := &\ \nu(\nabla(\boldsymbol{u}^* - \boldsymbol{u}_h^*), \nabla e^u) + \sigma(\boldsymbol{u}^* - \boldsymbol{u}_h^*, e^u) + (\nabla(p^* - p_h^*), e^u) - (e^p, \nabla\cdot(\boldsymbol{u}^* - \boldsymbol{u}_h^*)) \\ &- \sum_{K\in\mathcal{T}_h}\tau_K\Big(\sigma e^u - \nu\Delta e^u + \nabla e^p, \sigma(\boldsymbol{u}^* - \boldsymbol{u}_h^*) - \nu\Delta(\boldsymbol{u}^* - \boldsymbol{u}_h^*) + \nabla(p^* - p_h^*)\Big)_{0,K}.\end{aligned}$$

Following the argument for proving Lemma 3.2, we can obtain

$$\begin{aligned}|E| &\leq \frac{ch}{\sqrt{\nu}}\|(e^u, e^p)\|_h\Big(\nu|\boldsymbol{u}^*|_2 + |p^*|_1\Big) \\ &\quad + \frac{ch}{\sqrt{\nu}}\Big\{\Big(\sum_{K\in\mathcal{T}_h}h_K^2\nu\|\Delta(\boldsymbol{u} - \boldsymbol{I}_h\boldsymbol{u})\|_{0,K}^2\Big)^{1/2} + |\boldsymbol{I}_h\boldsymbol{u} - \boldsymbol{u}_h|_{1,\nu}\Big\}\Big(\nu|\boldsymbol{u}^*|_2 + |p^*|_1\Big),\end{aligned}$$

where the norm $\|(\cdot,\cdot)\|_h$ is given in (2.15) and the term $|\boldsymbol{I}_h\boldsymbol{u} - \boldsymbol{u}_h|_{1,\nu}$ satisfies (3.11). By the triangle inequality, we have

$$\|(e^u, e^p)\|_h \leq \|(\boldsymbol{u}, p) - (\boldsymbol{I}_h\boldsymbol{u}, J_hp)\|_h + \|(\boldsymbol{I}_h\boldsymbol{u}, J_hp) - (\boldsymbol{u}_h, p_h)\|_h,$$

where the second term in the right-hand side satisfies (3.11). From the finite element interpolation properties (3.1), (3.2), (3.3), (3.4) and (3.5) of $(\boldsymbol{I}_h \boldsymbol{u}, J_h p) \in \boldsymbol{V}_h \times Q_h$, we obtain

$$\|(\boldsymbol{u}, p) - (\boldsymbol{I}_h \boldsymbol{u}, J_h p)\|_h + \Big(\sum_{K\in\mathcal{T}_h} h_K^2 \nu \|\Delta(\boldsymbol{u} - \boldsymbol{I}_h \boldsymbol{u})\|_{0,K}^2\Big)^{1/2} \le c\Big(\sqrt{\nu} h^k |\boldsymbol{u}|_{k+1} + \frac{h^\ell}{\sqrt{\nu}} |p|_\ell\Big). \quad (4.3)$$

So, from (4.3), (3.11) and the regularity result (4.2), we have

$$\|e^u\|_0^2 \le c\Big(h^{k+1}|\boldsymbol{u}|_{k+1} + \frac{h^{\ell+1}}{4\nu/m}|p|_\ell\Big)\|e^u\|_0,$$

that is,

$$\|e^u\|_0 \le c\Big(h^{k+1}|\boldsymbol{u}|_{k+1} + \frac{h^{\ell+1}}{4\nu/m}|p|_\ell\Big).$$

We thus conclude the following result:

Lemma 4.1. *Under the same assumptions as in Lemma 3.2, assuming a convex Ω, we have*

$$\|\boldsymbol{u} - \boldsymbol{u}_h\|_0 \le c\Big(h^{k+1}|\boldsymbol{u}|_{k+1} + \frac{h^{\ell+1}}{4\nu/m}|p|_\ell\Big).$$

It is interesting that the above result, which is obtained mainly from Lemma 3.2, is *independent* of σ. To the authors' knowledge, such an estimate is new. In addition, we do not assume the quasi-uniform meshes.

Combining Corollary 3.1 and Lemma 4.1, we obtain the main result of the L^2 norm error bounds of the velocity when Ω is convex.

Theorem 4.1. *Under the same assumptions as in Corollary 3.1 and Lemma 4.1, we have*

$$\|\boldsymbol{u} - \boldsymbol{u}_h\|_0 \le c\Big(h^{k+1}|\boldsymbol{u}|_{k+1} + \frac{h^{\ell+1}}{\max\{\sigma h^2, 4\nu/m\}}|p|_\ell\Big).$$

As expected, such error estimates hold regardless of the values of σ and ν (Note that $\sigma = 0$ and $\nu = 0$ cannot hold simultaneously) and are one order higher than those in Theorem 3.1. Also, up to the regularity-norms of the exact solution pair $(\boldsymbol{u}, p)$, the L^2 norm error estimates no longer depend on ν, like the H^1 semi-norm error estimates, since $\max\{\sigma h^2, 4\nu/m\} \ge \sigma h^2$. Consequently, in a convex Ω, the convergence behaviors of both are the same with respect to σ and ν. Of course, relative to h, the former is one order higher the latter. In addition, for more regular pressure $p \in H^{\ell+1}(\Omega)$, we have

$$\|\boldsymbol{u} - \boldsymbol{u}_h\|_0 \le c\Big(h^{k+1}|\boldsymbol{u}|_{k+1} + \frac{h^{\ell+2}}{\max\{\sigma h^2, 4\nu/m\}}|p|_{\ell+1}\Big).$$

5. Discussions: Error Bounds for Numerical σ and ν

We have seen that the error estimates obtained are essentially uniform with respect to σ and ν. In this section, we shall consider the practical values among σ, ν and h and derive improved error estimates. We have not assumed the convexity of Ω in this section.

In practical computations, the mesh size h and σh^2 are relatively larger than ν. Note that σ and ν are inversely proportional to the time-step δt in the time discretization of the time-dependent Stokes problem and the Reynolds number Re, respectively. Two most interesting cases we shall consider, pertaining to the relationship among σ, h, ν and c, are as follows:

$$\sigma h^2 \geq c \geq \nu, \tag{5.1}$$

$$\sigma h \geq c \geq \nu/h. \tag{5.2}$$

Since σ and ν may not be changed for a specific problem while the mesh size h tends to zero, the values of σ and ν in (5.1) and (5.2) are only numerically meaningful, i.e., (5.1) and (5.2) hold only when h is not very small (as is exactly the realistic situation, however). With a glance at (5.1) and (5.2), they look alike. Indeed, from both (5.1) and (5.2) we have $\sigma h^2 \geq \nu$. But, $\nu \leq c$ in (5.1) while $\nu \leq ch$ is imposed in (5.2). The other difference is that when $\sigma^{-1} = c\delta t$ (time step), (5.2) means $\delta t \leq ch$ while (5.1) means $\delta t \leq ch^2$. Both (5.1) and (5.2) are generally fulfilled in the practical computations, anyway. In fact, for the time discretizations we choose either of the following two:

$$\delta t \leq ch^2, \quad \delta t \leq ch.$$

Such choices of the time step δt are quite common in time difference methods, e.g., see [36]. As for $\nu \leq c$ or $\nu \leq ch$, they are also practically true.

Now, we shall give the error estimates under (5.1) or (5.2). Under (5.1), from Theorem 3.1 we have

$$\|\nabla(\boldsymbol{u}-\boldsymbol{u}_h)\|_0 \leq c\big(h^k|\boldsymbol{u}|_{k+1} + h^\ell|p|_\ell\big), \quad \|\nabla(\boldsymbol{u}-\boldsymbol{u}_h)\|_0 \leq c\big(h^k|\boldsymbol{u}|_{k+1} + h^{\ell+1}|p|_{\ell+1}\big), \tag{5.3}$$

while, under (5.2), we have

$$\|\nabla(\boldsymbol{u}-\boldsymbol{u}_h)\|_0 \leq c\big(h^k|\boldsymbol{u}|_{k+1} + h^{\ell-1}|p|_\ell\big), \quad \|\nabla(\boldsymbol{u}-\boldsymbol{u}_h)\|_0 \leq c\big(h^k|\boldsymbol{u}|_{k+1} + h^\ell|p|_{\ell+1}\big), \tag{5.4}$$

In the above, we only need $\sigma h^2 \geq c$ or $\sigma h \geq c$ while $\nu \leq c$ and $\nu \leq ch$ are unnecessary, since the H^1 semi-norm errors of velocity do not depend on ν.

Under (5.1), from Corollary 3.1, we have

$$\|\boldsymbol{u}-\boldsymbol{u}_h\|_0 \leq c\big(h^{k+1}|\boldsymbol{u}|_{k+1} + h^{\ell+1}|p|_\ell\big). \tag{5.5}$$

Note that this is optimal with respect to the order of approximations and the regularity of the solution pair. Also, we do not require Ω to be convex or smooth, as is usually required in finite element analysis. If $p \in H^{\ell+1}(\Omega)$, we have

$$\|\boldsymbol{u}-\boldsymbol{u}_h\|_0 \leq c\big(h^{k+1}|\boldsymbol{u}|_{k+1} + h^{\ell+2}|p|_{\ell+1}\big). \tag{5.6}$$

Under (5.2), we have

$$\|\boldsymbol{u}-\boldsymbol{u}_h\|_0 \leq c\big(h^{k+1}|\boldsymbol{u}|_{k+1} + h^\ell|p|_\ell\big), \quad \|\boldsymbol{u}-\boldsymbol{u}_h\|_0 \leq c\big(h^{k+1}|\boldsymbol{u}|_{k+1} + h^{\ell+1}|p|_{\ell+1}\big). \tag{5.7}$$

Note that the error estimates for the pressure in H^1 semi-norm are independent of σ. Under the condition $\nu \leq c$ in (5.1), from Theorem 3.2 we have, for pressure in H^1 semi-norm,

$$\|\nabla(p_h - p)\|_0 \leq c\big(h^{\ell-1}|p|_\ell + h^{k-1}|\boldsymbol{u}|_{k+1}\big), \quad \|\nabla(p_h - p)\|_0 \leq c\big(h^\ell|p|_{\ell+1} + h^{k-1}|\boldsymbol{u}|_{k+1}\big). \tag{5.8}$$

Though not optimal relative to the order of approximations, such error estimates are classical in the standard Galerkin method. Under the condition $\nu \le ch$ in (5.2), we have

$$\|\nabla(p_h - p)\|_0 \le c\big(h^{\ell-1}|p|_\ell + h^k|\boldsymbol{u}|_{k+1}\big), \tag{5.9}$$

$$\|\nabla(p_h - p)\|_0 \le c\big(h^{\ell}|p|_{\ell+1} + h^k|\boldsymbol{u}|_{k+1}\big). \tag{5.10}$$

The error estimate (5.10) is unexpected at all. This means that, for smooth enough $\boldsymbol{u}$ and p, better approximations of the pressure will be produced under (5.2), with optimum in h with respect to the order of approximations. In the standard Galerkin method, in terms of the order of approximations, it is in general not possible to have optimal error estimates like (5.10) for the pressure.

6. Numerical Experiments

For testing the performance of the Barrenechea-Valentin stabilized FEM, remarkable numerical results have been reported in [3]. In this section, we are going to perform some further numerical experiments.

Example 6.1 (*A smooth solution problem*). In this example, we study an example taken from [4], defined on $\Omega = (0,1)\times(0,1)$, and examine the detailed convergence behavior of the stabilization method using P_1-P_1 finite elements. Assume that the smooth exact solution pair $(\boldsymbol{u}, p)$ of the generalized Stokes problem (1.1) is given by

$$\begin{cases} u_1(x,y) &= 2\pi x^2(1-x)^2\cos(\pi y)\sin(\pi y), \\ u_2(x,y) &= 2(1-x)(2x^2-x)\sin^2(\pi y), \\ p(x,y) &= \sin(x)\cos(y) + (\cos(1)-1)\sin(1). \end{cases} \tag{6.1}$$

Substituting the solution (6.1) into problem (1.1), we can obtain the source-like function $\boldsymbol{f}$. Notice that $\boldsymbol{u} = \boldsymbol{0}$ on $\partial\Omega$ and $\int_\Omega p = 0$. We first consider the uniform triangular meshes of Ω. A uniform triangular mesh is formed by dividing each square, with side-length h^* in a uniform square mesh, into two triangles by drawing a diagonal line from the left-down corner to the right-up corner. Therefore, we have $h_K = h = \sqrt{2}h^*$ for all $K \in \mathcal{T}_h$.

Numerical results produced by the stabilized FEM (2.8) for viscosity $\nu = 10^{-i}$, $i = 2,3,4$, and reaction coefficient $\sigma = 10^j$, $j = 0,1,\cdots,5$, are reported in Table 1 and Table 2, where the orders of convergence are estimated. The results of the classical Stokes problem, i.e., $\sigma = 0$, are also presented therein. We remark again that if $\sigma = 0$ then the element-wise stabilization parameter τ_K defined in (2.4) should be simplified to $\tau_K = h_K^2/(8\nu/m_k)$. From the numerical results, we have the following observations:

- For all considered values of the viscosity ν and the reaction coefficient σ, the stabilized FEM (2.8) displays optimal orders of convergence in the L^2 norm and H^1 norm for velocity field and in the H^1 norm for pressure. In the present paper, we do not give a new error estimate of pressure in the L^2 norm. However, from the error estimate (1.10) derived in [3], we can find that the convergence order of pressure in the L^2 norm is not optimal. This is also verified by the numerical results shown in Table 1.
- When $0 < \nu \ll 1$ and $\sigma \gg 1$, for a fixed mesh size h, the relative errors of velocity field $\boldsymbol{u}_h$ and pressure p_h in both the L^2 norm and H^1 norm appear to be uniform with respect to ν and σ. These results are consistent with the theoretical analysis given in this paper.

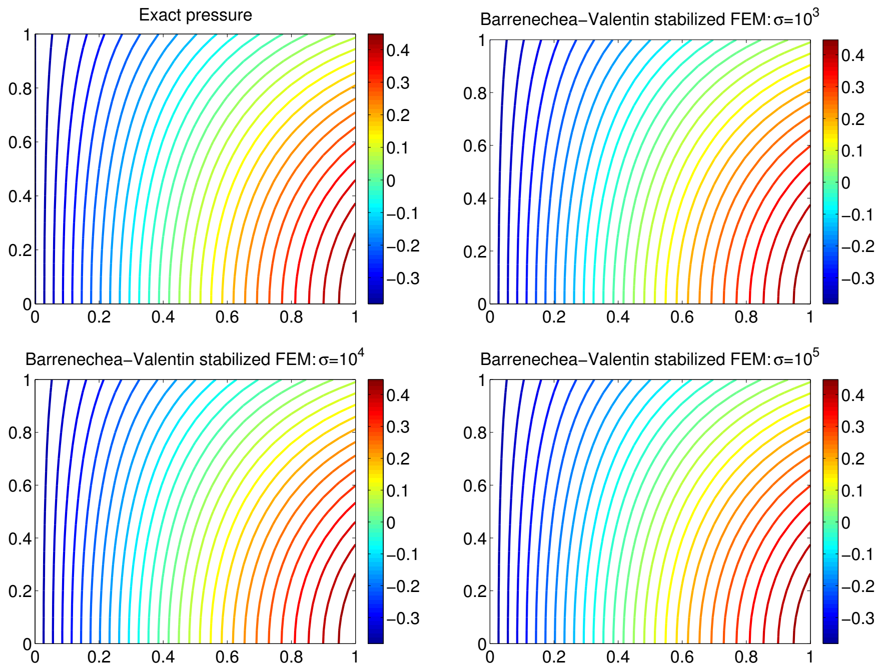

Figure 1: Contours of exact pressure and P_1 approximations on a uniform triangular mesh with $h^* = 1/20$, where $\nu = 10^{-3}$ and $\sigma = 10^3, 10^4, 10^5$

- The stabilized FEM (2.8) presents a robust behavior in the sense that no pressure instabilities appear, even if we use a rather coarse mesh with, e.g., $h^* = 1/20$; see Figure 1 for the contours of exact pressure and its approximations.

For further testing the effectiveness of the Barrenechea-Valentin stabilized FEM (2.8), we now consider the P_1-P_1 finite elements on an unstructured triangular mesh that is depicted in Figure 2. This mesh is constructed by dividing each side of the square Ω into equal segments with length $h^* = 1/20$ and then using the *FreeFem++* (see [29]) to generate an unstructured quasi-uniform mesh. The elevation plots of the exact and approximate solutions for $\nu = 10^{-3}$ and $\sigma = 10^5$ are shown in Figure 3. Again, one can find that the Barrenechea-Valentin stabilized FEM (2.8) generates stable and accurate results for $0 < \nu \ll 1$ and $\sigma \gg 1$, even if we use a rather coarse mesh with $h^* = 1/20$.

Example 6.2 (*A time-dependent lid-driven cavity flow*). We consider a lid-driven cavity flow problem governed by the following time-dependent, incompressible Stokes equations (cf. [2]):

$$\left\{ \begin{array}{rcll} \dfrac{\partial \boldsymbol{u}}{\partial t} - \nu\Delta\boldsymbol{u} + \nabla p & = & \boldsymbol{0} & \text{in } I \times \Omega, \\ \nabla\cdot\boldsymbol{u} & = & 0 & \text{in } I \times \Omega, \\ \boldsymbol{u} & = & \boldsymbol{0} & \text{on } \bar{I} \times (\partial\Omega \setminus ([0,1] \times \{1\})), \\ \boldsymbol{u} & = & (1,0)^\top & \text{on } \bar{I} \times ([0,1] \times \{1\}), \\ \boldsymbol{u} & = & \boldsymbol{0} & \text{on } \{0\} \times \Omega, \end{array} \right. \tag{6.2}$$

where the time interval and the spatial domain are given by $I = (0,T)$ with $T > 0$ and $\Omega = (0,1) \times (0,1)$, respectively. The boundary conditions for $t \in [0,T]$ are depicted in Figure 4.

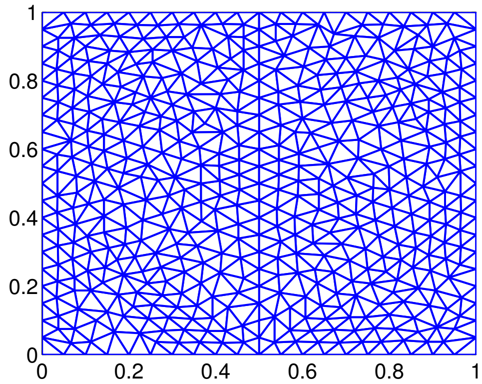

Figure 2: An unstructured triangular mesh with $h^* = 1/20$

Let the time interval $[0, T]$ be uniformly partitioned into l subintervals by $\{0 = t_0 < t_1 < \cdots < t_{l-1} < t_l = T\}$ with a constant time step $\delta t = t_n - t_{n-1}$ for $n = 1, 2, \cdots, l$. Then we set $\sigma = 1/\delta t$. For any $n \geq 1$, we denote the approximate solutions at time level n by $\boldsymbol{u}_h^n$ and p_h^n. The time discretization is performed by using the first-order backward Euler scheme and the spatial discretization is carried out by employing the stabilized FEM (2.8) with P_1-P_1 finite elements on a uniform triangular mesh as that described in Example 6.1. Then we have the following fully discrete problem at time level n: find $(\boldsymbol{u}_h^n, p_h^n)$ such that

$$\begin{aligned}\sigma(\boldsymbol{u}_h^n, \boldsymbol{v}_h) + \nu(\nabla \boldsymbol{u}_h^n, \nabla \boldsymbol{v}_h) - (p_h^n, \nabla \cdot \boldsymbol{v}_h) - (q_h, \nabla \cdot \boldsymbol{u}_h^n)& \\ - \sum_{K \in \mathcal{T}_h} \tau_K(\sigma \boldsymbol{u}_h^n - \nu \Delta \boldsymbol{u}_h^n + \nabla p_h^n, \sigma \boldsymbol{v}_h - \nu \Delta \boldsymbol{v}_h + \nabla q_h)_{0,K}& \\ = (\sigma \boldsymbol{u}_h^{n-1}, \boldsymbol{v}_h) - \sum_{K \in \mathcal{T}_h} \tau_K(\sigma \boldsymbol{u}_h^{n-1}, \sigma \boldsymbol{v}_h - \nu \Delta \boldsymbol{v}_h + \nabla q_h)_{0,K},& \qquad (6.3)\end{aligned}$$

for all $(\boldsymbol{v}_h, q_h) \in \mathcal{V}_h \times \mathcal{Q}_h$, where $\boldsymbol{u}_h^n$ is required to satisfy the prescribed boundary conditions.

We consider the case $\nu = 10^{-3}$, $\delta t = 10^{-3}$ $(\sigma = 10^3)$ and $h^* = 1/40$ and perform the simulation of the stabilized FEM (6.3) to reach a steady-state solution. The stopping criterion for the time advancing is given by

$$\|\boldsymbol{u}_h^n - \boldsymbol{u}_h^{n-1}\|_0 < 10^{-5} \|\boldsymbol{u}_h^n\|_0.$$

The contours of stream function and pressure at the steady state time $T = 0.985$ are shown in Figure 5. From the numerical results shown in Figure 5, we can find that the stabilized FEM (6.3) produces a reasonable result with a high stability.

Next, we consider a time-independent lid-driven cavity flow problem. We solve the generalized Stokes equations (1.1), with the boundary conditions described in Figure 4, using P_1-P_1 finite elements on a uniform triangular mesh of mesh size $h^* = 1/20$. We depict a vertical cross section of the velocity component u_1 for $\nu = 10^{-3}$ and $\sigma = 10^3$ in Figure 6. In this test, we can observe the presence of a strong boundary layer on the velocity that is well recovered by the stabilized FEM (2.8), even we use a rather coarse mesh.

7. Conclusion

In this paper, we have derived sharper stability and error estimates of the Barrenechea-Valentin stabilized FEM using the $\mathcal{C}^0$ elements for both velocity and pressure. We have explicitly established the dependence of stability and error bounds on the viscosity ν, the reaction constant σ, and the mesh parameter h. It is revealed that the viscosity constant ν and the reaction constant σ respectively act in the numerator position and the denominator position in the error estimates of velocity and pressure in standard norms without any weights. Error estimates for a convex domain of the velocity are also obtained. For numerically interesting situations, we have derived improved error estimates, which are uniform with respect to σ and ν (up to the regularity-norms of the exact solution pair). All these error estimates support that the Barrenechea-Valentin method is indeed suitable for the generalized Stokes problem with a small viscosity ν and a large reaction coefficient σ, in the sense of (5.1) or (5.2). These error estimates obtained agree very well with the numerical experiments. Such sharper *a priori* stability and error estimates have not been achieved elsewhere and before. It will be interesting if similar results can hold for the general time-dependent incompressible Navier-Stokes equations. This work is ongoing and will be reported elsewhere in the near future.

Acknowledgments. The authors would like to thank the anonymous referees for their valuable comments and suggestions that led to a substantial improvement of the paper. The work of H.-Y. Duan was supported by the National Natural Science Foundation of China under grants 11571266, 11661161017, 11171168, 11071132, the Collaborative Innovation Centre of Mathematics, and the Computational Science Hubei Key Laboratory (Wuhan University). The work of P.-W. Hsieh was supported by the Ministry of Science and Technology of Taiwan under grants MOST 104-2811-M-008-049 and MOST 106-2115-M-005-005-MY2. The work of S.-Y. Yang was supported by the Ministry of Science and Technology of Taiwan under grants MOST 103-2115-M-008-009-MY3 and MOST 106-2115-M-008-014-MY2.

References

[1] R. Araya, G. R. Barrenechea, and F. Valentin, Stabilized finite element methods based on multiscale enrichment for the Stokes problem, *SIAM J. Numer. Anal.*, **44** (2006), 322-348.

[2] G. R. Barrenechea and J. Blasco, Pressure stabilization of finite element approximations of time-dependent incompressible flow problems, *Comput. Methods Appl. Mech. Engrg.*, **197** (2007), 219-231.

[3] G. R. Barrenechea and F. Valentin, An unusual stabilized finite element method for a generalized Stokes problem, *Numer. Math.*, **92** (2002), 653-677.

[4] P. B. Bochev, M. D. Gunzburger, and R. B. Lehoucq, On stabilized finite element methods for the Stokes problem in the small time step limit, *Int. J. Numer. Meth. Fluids,* **53** (2007), 573-597.

[5] P. B. Bochev, M. D. Gunzburger, and J. N. Shadid, On inf-sup stabilized finite element methods for transient problems, *Comput. Methods Appl. Mech. Engrg.*, **193** (2004), 1471-1489.

[6] M. Braack and G. Lube, Finite elements with local projection stabilization for incompressible flow problems, *J. Comput. Math.*, **27** (2009), 116-147.

[7] M. Braack, E. Burman, V. John, and G. Lube, Stabilized finite element methods for the generalized Oseen problem, *Comput. Methods Appl. Mech. Engrg.*, **196** (2007), 853-866.

[8] S. C. Brenner and L. R. Scott, *The Mathematical Theory of Finite Element Methods,* Springer-Verlag, New York, 1994.

[9] F. Brezzi and J. Douglas Jr., Stabilized mixed methods for the Stokes problem, *Numer. Math.,* **53** (1988), 225-235.

[10] F. Brezzi and M. Fortin, *Mixed and Hybrid Finite Element Methods,* Springer-Verlag, New York, 1991.

[11] F. Brezzi and J. Pitkäranta, On the stabilization of finite element approximations of the Stokes problem, in: W. Hackbush, editor, *Efficient Solution of Elliptic Systems, Notes on Numerical Fluid Mechanics, Vol. 10,* pp. 11-19, Braunschweig, Wiesbaden, Viewig, 1984.

[12] A. N. Brooks and T. J. R. Hughes, Streamline upwind/Petrov-Galerkin formulations for convection dominated flows with a particular emphasis on the incompressible Navier-Stokes equations, *Comput. Methods Appl. Mech. Engrg.,* **32** (1982), 199-259.

[13] P. G. Ciarlet, Basic error estimates for elliptic problems, in: P. G. Ciarlet and J.-L. Lions eds, *Handbook of Numerical Analysis, Vol. II, Finite Element Methods (part 1),* North-Holland, Amsterdam, 1991.

[14] A. L. G. A. Coutinho, L. P. Franca, and F. Valentin, Simulating transient phenomena via residual free bubbles, *Comput. Methods Appl. Mech. Engrg.,* **200** (2011), 2127-2130.

[15] J. Douglas, Jr. and J. Wang, An absolutely stabilized finite element method for the Stokes problem, *Math. Comput.,* **52** (1989), 495-508.

[16] H.-Y. Duan, P.-W. Hsieh, R. C. E. Tan, and S.-Y. Yang, Analysis of a new stabilized finite element method for the reaction-convection-diffusion equations with a large reaction coefficient, *Comput. Methods Appl. Mech. Engrg.,* **247-248** (2012), 15-36.

[17] H.-Y. Duan, P.-W. Hsieh, R. C. E. Tan, and S.-Y. Yang, Analysis of the small viscosity and large reaction coefficient in the computation of the generalized Stokes problem by a novel stabilized finite element method, *Comput. Methods Appl. Mech. Engrg.,* **271** (2014), 23-47.

[18] H. C. Elman, D. J. Silvester, and A. J. Wathen, *Finite Elements and Fast Iterative Solvers: with Applications in Incompressible Fluid Dynamics,* Oxford University Press, New York, 2005.

[19] H. Fernando, C. Harder, D. Paredes, and F. Valentin, Numerical multiscale methods for a reaction dominated model, *Comput. Methods Appl. Mech. Engrg.,* **201-204** (2012), 228-244.

[20] L. P. Franca and C. Farhat, Bubble functions prompt unusual stabilized finite element methods, *Comput. Methods Appl. Mech. Engrg.,* **123** (1995), 299-308.

[21] L. P. Franca, S. L. Frey, and T. J. R. Hughes, Stabilized finite element methods: I. application to the advective-diffusive model, *Comput. Methods Appl. Mech. Engrg.,* **95** (1992), 253-276.

[22] L. P. Franca and S. L. Frey, Stabilized finite element methods: II. the incompressible Navier-Stokes equations, *Comput. Methods Appl. Mech. Engrg.,* **99** (1992), 209-233.

[23] L. P. Franca and F. Valentin, On an improved unusual stabilized finite element method for the advective-reactive-diffusive equation, *Comput. Methods Appl. Mech. Engrg.,* **190** (2000), 1785-1800.

[24] L. P. Franca, V. John, G. Matthies, and L. Tobiska, An inf-sup stable and residual-free bubble element for the Oseen equations, *SIAM J. Numer. Anal.,* **45** (2007), 2392-2407.

[25] V. Girault and P. A. Raviart, *Finite Element Methods for Navier-Stokes Equations: Theory and Algorithms,* Springer-Verlag, New York, 1986.

[26] J.-L. Guermond, A. Marra, and L. Quartapelle, Subgrid stabilized projection method for 2D unsteady flows at high Reynolds numbers, *Comput. Methods Appl. Mech. Engrg.,* **195** (2006), 5857-5876.

[27] E. Hachem, B. Rivaux, T. Kloczko, H. Digonnet, and T. Coupez, Stabilized finite element method for incompressible flows with high Reynolds number, *J. Comput. Phys.,* **229** (2010), 8643-8665.

[28] I. Harari and T. J. R. Hughes, What are C and h?: inequalities for the analysis and design of finite element methods, *Comput. Methods Appl. Mech. Engrg.,* **97** (1992), 157-192.

[29] F. Hecht, O. Pironneau, J. Morice, A. Le Hyaric, and K. Ohtsuka, *FreeFem++, Third Edition, Version 3.19,* 2012, http://www.freefem.org/ff++/.

[30] P.-W. Hsieh and S.-Y. Yang, A new stabilized linear finite element method for solving reaction-convection-diffusion equations, *Comput. Methods Appl. Mech. Engrg.,* **307** (2016), 362-382.

[31] M.-C. Hsu, Y. Bazilevs, V. M. Calo, T. E. Tezduyar, and T. J. R. Hughes, Improving stability of stabilized and multiscale formulations in flow simulations at small time steps, *Comput. Methods Appl. Mech. Engrg.,* **199** (2010), 828-840.

[32] T. J. R. Hughes and L. P. Franca, A new finite element formulation for computational fluid dynamics: VII. The Stokes problem with various well-posed boundary conditions: symmetric formula-

tions that converge for all velocity/pressure spaces, *Comput. Methods Appl. Mech. Engrg.*, **65** (1987), 85-96.

[33] T. J. R. Hughes, L. P. Franca, and M. Balestra, A new finite element formulation for computational fluids dynamics: V. Circumventing the Babuška-Brezzi condition: a stable Petrov-Galerkin formulation of the Stokes problem accommodating equal-order interpolations, *Comput. Methods Appl. Mech. Engrg.*, **59** (1986), 85-99.

[34] K. Nafa and A. J. Wathen, Local projection stabilized Galerkin approximations for the generalized Stokes problem, *Comput. Methods Appl. Mech. Engrg.*, **198** (2009), 877-883.

[35] E. Oñate, A. Valls, and J. García, Modeling incompressible flows at low and high Reynolds numbers via a finite calculus-finite element approach, *J. Comput. Phys.*, **224** (2007), 332-351.

[36] A. Quarteroni and A. Valli, *Numerical Approximation of Partial Differential Equations*, Springer-Verlag, Berlin, 1994.

[37] H.-G. Roos, M. Stynes, L. Tobiska, *Robust Numerical Methods for Singularly Perturbed Differential Equations: Convection-Diffusion-Reaction and Flow Problems, Second Edition*, Springer-Verlag, Berlin, 2008.

[38] V. Thomée, *Galerkin Finite Element Methods for Parabolic Problems, Second Edition*, Springer-Verlag, Berlin, 2006.

[39] L. Tobiska, Recent results on local projection stabilization for convection-diffusion and flow problems, in: BAIL 2008-Boundary and Interior Layers, A. F. Hegarty et al., eds., *Lecture Notes in Computational Science and Engineering, Vol. 69*, pp. 55-75, Springer-Verlag, Berlin Heidelberg, 2009.

[40] L. Tobiska and R. Verfürth, Analysis of a streamline diffusion finite element method for the Stokes and Navier-Stokes equations, *SIAM J. Numer. Anal.*, **33** (1996), 107-127.

Table 1: L^2 relative errors of $\boldsymbol{u}_h$ and p_h for various values of the viscosity ν and the reaction coefficient σ

ν	σ	$h^* = 1/20$	$1/40$	$1/60$	$1/80$	$1/100$	order
L^2 relative errors of $\boldsymbol{u}_h$							
10^{-2}	0	1.8076e-2	4.5534e-3	2.0266e-3	1.1405e-3	7.3010e-4	2.00
	1	1.5617e-2	3.8766e-3	1.7206e-3	9.6738e-4	6.1898e-4	2.00
	10^1	1.6782e-2	3.6577e-3	1.5888e-3	8.8668e-4	5.6542e-4	2.07
	10^2	2.4697e-2	6.2792e-3	1.9085e-3	9.6719e-4	5.9276e-4	2.37
	10^3	2.4726e-2	6.2875e-3	2.8091e-3	1.5841e-3	1.0153e-3	1.99
	10^4	2.4728e-2	6.2879e-3	2.8092e-3	1.5842e-3	1.0154e-3	1.99
	10^5	2.4728e-2	6.2879e-3	2.8092e-3	1.5842e-3	1.0154e-3	1.99
10^{-3}	0	1.8228e-2	4.5559e-3	2.0268e-3	1.1405-3	7.3010e-4	2.00
	1	1.7009e-2	3.6668e-3	1.5903e-3	8.8710e-4	5.6558e-4	2.08
	10^1	2.4744e-2	6.2886e-3	1.9104e-3	9.6776e-4	5.9299e-4	2.37
	10^2	2.4730e-2	6.2890e-3	2.8097e-3	1.5844e-3	1.0155e-3	1.99
	10^3	2.4729e-2	6.2880e-3	2.8093e-3	1.5842e-3	1.0154e-3	1.99
	10^4	2.4728e-2	6.2879e-3	2.8092e-3	1.5842e-3	1.0154e-3	1.99
	10^5	2.4728e-2	6.2879e-3	2.8092e-3	1.5842e-3	1.0154e-3	1.99
10^{-4}	0	3.0146e-2	4.8533e-3	2.0559e-3	1.1459e-3	7.3153e-4	2.20
	1	2.6155e-2	6.5167e-3	1.9526e-3	9.7869e-4	5.9680e-4	2.40
	10^1	2.4787e-2	6.3072e-3	2.8177e-3	1.5885e-3	1.0178e-3	1.99
	10^2	2.4733e-2	6.2895e-3	2.8100e-3	1.5846e-3	1.0157e-3	1.99
	10^3	2.4729e-2	6.2881e-3	2.8093e-3	1.5842e-3	1.0154e-3	1.99
	10^4	2.4728e-2	6.2879e-3	2.8092e-3	1.5842e-3	1.0154e-3	1.99
	10^5	2.4728e-2	6.2879e-3	2.8092e-3	1.5842e-3	1.0154e-3	1.99
L^2 relative errors of p_h							
10^{-2}	0	5.7335e-4	1.4158e-4	6.2748e-5	3.5257e-5	2.2552e-5	2.01
	1	5.5464e-4	1.3636e-4	6.0435e-5	3.3960e-5	2.1724e-5	2.01
	10^1	8.3572e-4	1.6858e-4	7.4446e-5	4.1904e-5	2.6841e-5	2.08
	10^2	2.6269e-3	8.3644e-4	2.1699e-4	1.0815e-4	6.7290e-5	2.38
	10^3	2.9713e-3	1.2086e-3	7.1037e-4	4.7589e-4	3.4133e-4	1.37
	10^4	3.0129e-3	1.2767e-3	7.9725e-4	5.7427e-4	4.4512e-4	1.17
	10^5	3.0163e-3	1.2841e-3	8.0761e-4	5.8745e-4	4.6095e-4	1.14
10^{-3}	0	5.2546e-4	1.2968e-4	5.7494e-5	3.2312e-5	2.0671e-5	2.01
	1	6.0917e-4	1.3151e-4	5.7770e-5	3.2416e-5	2.0729e-5	2.06
	10^1	1.1619e-3	2.4183e-4	7.1359e-5	3.5789e-5	2.2120e-5	2.46
	10^2	1.3193e-3	3.5527e-4	1.6383e-4	9.3299e-5	5.9560e-5	1.94
	10^3	1.3386e-3	3.7751e-4	1.8648e-4	1.1518e-4	8.0063e-5	1.72
	10^4	1.3404e-3	3.7994e-4	1.8922e-4	1.1819e-4	8.3297e-5	1.69
	10^5	1.3382e-3	3.8016e-4	1.8950e-4	1.1850e-4	8.3639e-5	1.68
10^{-4}	0	5.2451e-4	1.2951e-4	5.7429e-5	3.2278e-5	2.0650e-5	2.01
	1	1.0439e-3	1.9839e-4	6.5129e-5	3.3730e-5	2.1043e-5	2.39
	10^1	1.1824e-3	2.8569e-4	1.1907e-4	6.1812e-5	3.6321e-5	2.22
	10^2	1.1996e-3	3.0346e-4	1.3547e-4	7.6221e-5	4.8617e-5	2.00
	10^3	1.2014e-3	3.0541e-4	1.3749e-4	7.8251e-5	5.0642e-5	1.96
	10^4	1.2013e-3	3.0561e-4	1.3769e-4	7.8462e-5	5.0857e-5	1.96
	10^5	1.1986e-3	3.0558e-4	1.3771e-4	7.8482e-5	5.0879e-5	1.96

Table 2: H^1 relative errors of $\boldsymbol{u}_h$ and p_h for various values of the viscosity ν and the reaction coefficient σ

ν	σ	$h^* = 1/20$	1/40	1/60	1/80	1/100	order
H^1 relative errors of $\boldsymbol{u}_h$							
10^{-2}	0	1.3194e-1	6.6200e-2	4.4162e-2	3.3129e-2	2.6506e-2	1.00
	1	1.3200e-1	6.6210e-2	4.4165e-2	3.3130e-2	2.6507e-2	1.00
	10^1	1.3222e-1	6.6243e-2	4.4176e-2	3.3135e-2	2.6509e-2	1.00
	10^2	1.3297e-1	6.6421e-2	4.4192e-2	3.3141e-2	2.6512e-2	1.00
	10^3	1.3300e-1	6.6442e-2	4.4264e-2	3.3184e-2	2.6540e-2	1.00
	10^4	1.3300e-1	6.6445e-2	4.4267e-2	3.3187e-2	2.6542e-2	1.00
	10^5	1.3300e-1	6.6445e-2	4.4267e-2	3.3187e-2	2.6543e-2	1.00
10^{-3}	0	1.3213e-1	6.6206e-2	4.4163e-2	3.3129e-2	2.6506e-2	1.00
	1	1.3238e-1	6.6249e-2	4.4176e-2	3.3135e-2	2.6509e-2	1.00
	10^1	1.3301e-1	6.6428e-2	4.4192e-2	3.3141e-2	2.6512e-2	1.00
	10^2	1.3300e-1	6.6443e-2	4.4265e-2	3.3184e-2	2.6540e-2	1.00
	10^3	1.3300e-1	6.6445e-2	4.4267e-2	3.3187e-2	2.6543e-2	1.00
	10^4	1.3300e-1	6.6445e-2	4.4267e-2	3.3187e-2	2.6543e-2	1.00
	10^5	1.3300e-1	6.6445e-2	4.4267e-2	3.3187e-2	2.6543e-2	1.00
10^{-4}	0	1.4855e-1	6.6719e-2	4.4229e-2	3.3145e-2	2.6511e-2	1.04
	1	1.3451e-1	6.6728e-2	4.4245e-2	3.3155e-2	2.6517e-2	1.01
	10^1	1.3305e-1	6.6461e-2	4.4273e-2	3.3189e-2	2.6542e-2	1.00
	10^2	1.3300e-1	6.6446e-2	4.4268e-2	3.3187e-2	2.6543e-2	1.00
	10^3	1.3300e-1	6.6446e-2	4.4267e-2	3.3187e-2	2.6543e-2	1.00
	10^4	1.3300e-1	6.6445e-2	4.4267e-2	3.3187e-2	2.6543e-2	1.00
	10^5	1.3300e-1	6.6445e-2	4.4267e-2	3.3187e-2	2.6543e-2	1.00
H^1 relative errors of p_h							
10^{-2}	0	2.3215e-2	1.1619e-2	7.7475e-3	5.8110e-3	4.6490e-3	1.00
	1	2.3209e-2	1.1619e-2	7.7474e-3	5.8110e-3	4.6490e-3	1.00
	10^1	2.3264e-2	1.1623e-2	7.7487e-3	5.8115e-3	4.6492e-3	1.00
	10^2	2.3946e-2	1.2205e-2	7.8434e-3	5.8400e-3	4.6609e-3	1.02
	10^3	2.4021e-2	1.2314e-2	8.3723e-3	6.3887e-3	5.1926e-3	0.95
	10^4	2.4031e-2	1.2337e-2	8.4072e-3	6.4338e-3	5.2452e-3	0.94
	10^5	2.4034e-2	1.2339e-2	8.4115e-3	6.4401e-3	5.2537e-3	0.94
10^{-3}	0	2.3211e-2	1.1619e-2	7.7475e-3	5.8110e-3	4.6490e-3	1.00
	1	2.3189e-2	1.1618e-2	7.7473e-3	5.8110e-3	4.6490e-3	1.00
	10^1	2.3171e-2	1.1618e-2	7.7471e-3	5.8109e-3	4.6490e-3	1.00
	10^2	2.3172e-2	1.1618e-2	7.7513e-3	5.8158e-3	4.6540e-3	1.00
	10^3	2.3172e-2	1.1619e-2	7.7518e-3	5.8164e-3	4.6547e-3	1.00
	10^4	2.3173e-2	1.1619e-2	7.7519e-3	5.8165e-3	4.6548e-3	1.00
	10^5	2.3173e-2	1.1619e-2	7.7519e-3	5.8165e-3	4.6548e-3	1.00
10^{-4}	0	2.3212e-2	1.1619e-2	7.7475e-3	5.8110e-3	4.6490e-3	1.00
	1	2.3164e-2	1.1612e-2	7.7463e-3	5.8107e-3	4.6489e-3	1.00
	10^1	2.3163e-2	1.1611e-2	7.7450e-3	5.8099e-3	4.6484e-3	1.00
	10^2	2.3163e-2	1.1611e-2	7.7449e-3	5.8099e-3	4.6484e-3	1.00
	10^3	2.3163e-2	1.1611e-2	7.7449e-3	5.8099e-3	4.6484e-3	1.00
	10^4	2.3163e-2	1.1611e-2	7.7449e-3	5.8099e-3	4.6484e-3	1.00
	10^5	2.3163e-2	1.1611e-2	7.7449e-3	5.8099e-3	4.6484e-3	1.00

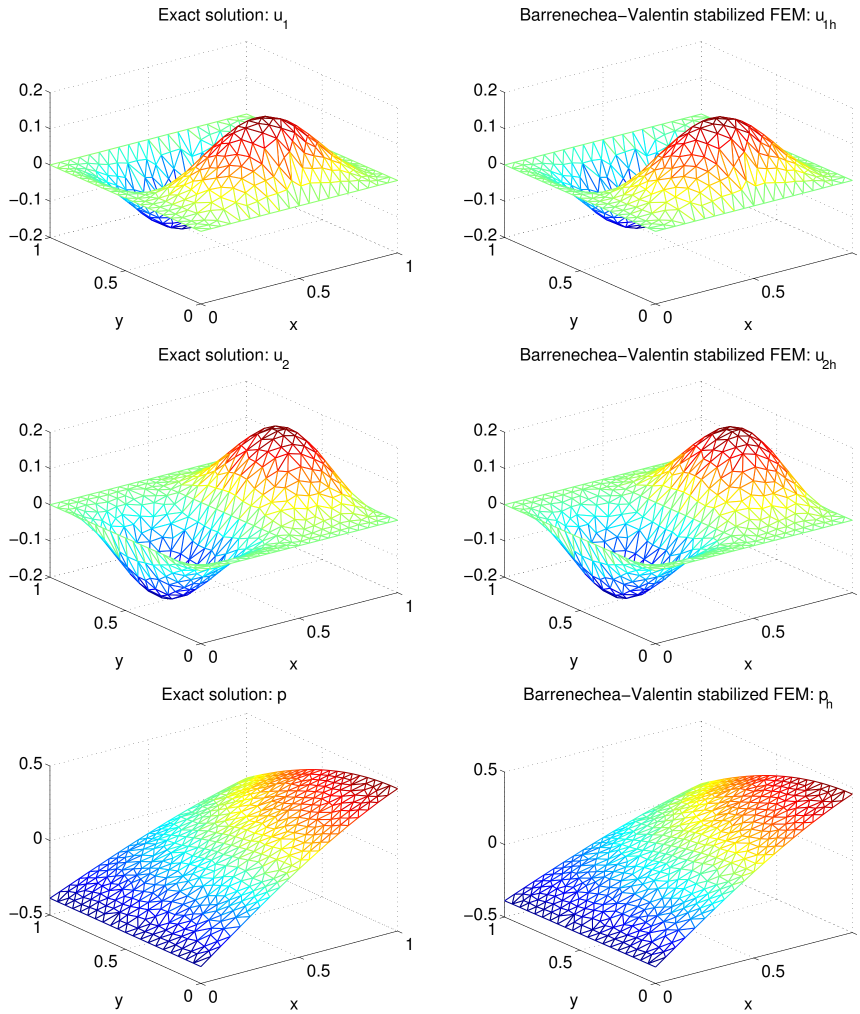

Figure 3: Elevation plots of the exact solutions and the approximate solutions on an unstructured triangular mesh with $h^* = 1/20$, where $\nu = 10^{-3}$ and $\sigma = 10^5$

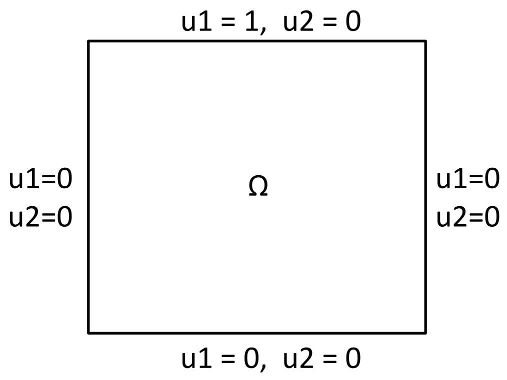

Figure 4: Statement of the boundary conditions of the lid-driven cavity flow problem for $t \in [0, T]$.

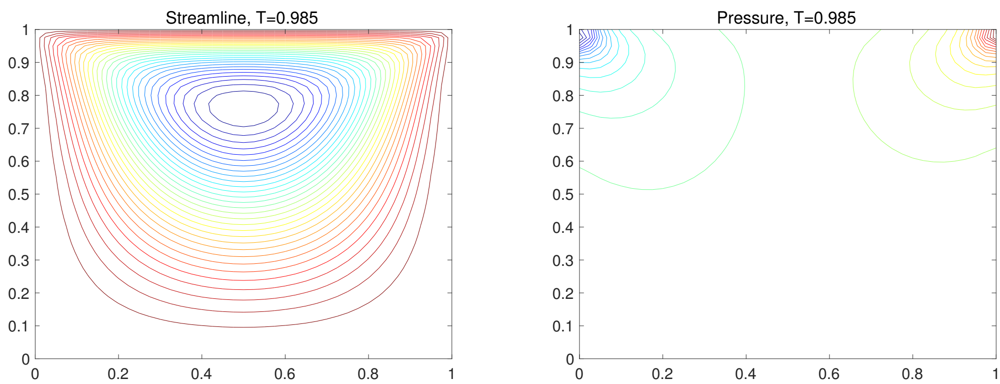

Figure 5: Contours of stream function and pressure at the steady state produced by the Barrenechea-Valentin stabilized FEM (2.8) on a uniform triangular mesh with $h^* = 1/40$ for the time-dependent lid-driven cavity flow problem, where $\nu = 10^{-3}$ and $\delta t = 10^{-3}$ ($\sigma = 10^3$).

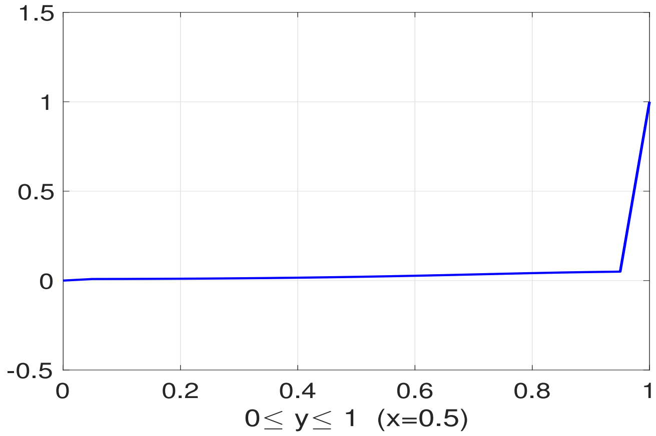

Figure 6: Vertical cross section of the velocity component u_1 at $x = 0.5$ of the time-independent lid-driven cavity flow problem with $\nu = 10^{-3}$ and $\sigma = 10^3$, where $h^* = 1/20$.